Developmental Biology
Chromosomes and Gene Expression

Complex aneuploidy triggers autophagy and p53-mediated apoptosis and impairs the second lineage segregation in human preimplantation embryos

Reviewed Preprint
v2 • November 21, 2024
Revised by authors

Reviewed Preprint
v1 • September 8, 2023

Marius Regin, Yingnan Lei, Edouard Couvreu De Deckersberg, Charlotte Janssens, Anfien Huyghebaert, Yves Guns, Pieter Verdyck, Greta Verheyen, Hilde Van de Velde, Karen Sermon, Claudia Spits

Research Group Genetics Reproduction and Development, Faculty of Medicine and Pharmacy, Vrije Universiteit Brussel, Brussels, Belgium • Brussels IVF, Universitair Ziekenhuis Brussel, Brussels, Belgium • Vrije Universiteit Brussel (VUB), Universitair Ziekenhuis Brussel (UZ Brussel), Clinical Sciences, Research Group Genetics Reproduction and Development, Centre for Medical Genetics, Brussels, Belgium

eLife Assessment

This study provides **valuable** insights into the cellular responses to complex aneuploidy in human preimplantation embryos. The evidence supporting the claims of the authors is now **convincing** after addressing previous concerns. This work will be of interest to embryologists, geneticists and scholars working on reproductive medicine by increasing our understanding of how human embryos respond to chromosomal abnormalities.

https://doi.org/10.7554/eLife.88916.2.sa3

Abstract

About 70% of human cleavage stage embryos show chromosomal mosaicism, falling to 20% in blastocysts. Chromosomally mosaic human blastocysts can implant and lead to healthy new-borns with normal karyotypes. Studies in mouse embryos and human gastruloids have shown that aneuploid cells show proteotoxic stress, autophagy and p53 activation and that they are eliminated from the epiblast by apoptosis while being tolerated in the trophectoderm. These observations suggest a selective loss of aneuploid cells from human embryos, but the underlying mechanisms are not yet fully understood. In this study we investigated the cellular consequences of aneuploidy in a total of 125 human blastocysts. RNA-sequencing of trophectoderm cells showed transcriptional signatures of activated p53 pathway and apoptosis, which was proportionate to the level of chromosomal imbalance. Immunostaining corroborated that aneuploidy triggers proteotoxic stress, autophagy, p53-signalling, and apoptosis independent from DNA damage. Total cell numbers were lower in aneuploid embryos, due to a decline both in trophectoderm and in epiblast/primitive

endoderm cell numbers. While lower cell numbers in trophectoderm may be attributed to apoptosis, it appeared that aneuploidy impaired the second lineage segregation, particularly primitive endoderm formation. This might be reinforced by retention of NANOG in aneuploid embryos. Our findings might explain why fully aneuploid embryos fail to further develop and we hypothesize that the same mechanisms lead to removal of aneuploid cells from mosaic embryos. This hypothesis needs further study as we did not analyze chromosomal mosaic embryos. Finally, we demonstrated a few differences with previous findings in the mouse, emphasizing the need for human embryo research to understand the consequences of aneuploidy.

Introduction

Aneuploidy is common in human preimplantation embryos from both natural (Munné et al., 2020a) and medically assisted reproduction cycles (Capalbo et al., 2021; Chavez et al., 2012; Chow et al., 2014; Fragouli et al., 2019; Johnson et al., 2010; Mertzanidou et al., 2013b, 2013a; Popovic et al., 2020; Starostik et al., 2020; Vanneste et al., 2009; Voullaire et al., 2000; Wells and Delhanty, 2000; Yang et al., 2021). Depending on the study, up to 80% of human cleavage stage embryos are found to be aneuploid, of which 70% show chromosomal mosaicism, i.e., the presence of at least two cell lineages with different genomic content (Regin et al., 2022). The reasons behind this high rate of chromosomal abnormalities of mitotic origin is still largely unknown (McCoy, 2017). One explanation is that cleavage-stage embryos have a weak spindle assembly checkpoint (SAC) that is uncoupled of apoptosis until the blastocyst stage (Jacobs et al., 2017; Vázquez-Diez et al., 2019), in combination with an abundancy of transcripts of anti-apoptotic genes (Yan et al., 2013). Only after embryonic genome activation, the rapidly increasing expression of pro-apoptotic genes along with the full functionality of the SAC establishes the control of mitotic errors. Additionally, aneuploidy in human embryos originates from an erroneous first mitotic division through a prolonged prometaphase (Currie et al., 2022).

It is by now well established that chromosomally mosaic embryos can result in healthy new-borns with normal karyotypes, implying a progressive and selective loss of aneuploid cells during development (Capalbo et al., 2021; Fragouli et al., 2019, 2017; Greco et al., 2015; Munné et al., 2020b, 2017; Viotti et al., 2021; Yang et al., 2021). In the preimplantation embryo, several studies have shown that the proportion of aneuploid cells within the embryo decreases as from three days post fertilization (3dpf) (Fragouli et al., 2019; van Echten-Arends et al., 2011; Yang et al., 2021) with no apparent preferential allocation of aneuploid cells to either trophectoderm (TE) or inner cell mass (ICM) (Capalbo et al., 2013; Popovic et al., 2018; Ren et al., 2022; Starostik et al., 2020). Conversely, the TE of mouse embryos treated with the SAC inhibitor reversine show a similar but statistically significant 6% enrichment for aneuploid cells (Bolton et al., 2016). Similarly, other studies on human embryos found that the TE contained a slightly higher number of aneuploid cells than the ICM, but without reaching statistical significance (Griffin et al., 2022; Starostik et al., 2020). Lastly, aneuploid cells have also been found to be excluded as cell debris (Orvieto et al., 2020) or allocated to the blastocoel cavity and to peripheral cells that do not participate in the formation of the embryo (Griffin et al., 2022).

After implantation, aneuploid cells become progressively more frequent in the trophoblast lineage as compared to the epiblast (EPI) and primitive endoderm (PrE) (Starostik et al., 2020). This suggests that the trophoblast cells are more tolerant to aneuploidy, which is in line with the rate of 1-2% of confined placental mosaicism found in the general population (Kalousek and Vekemans, 1996). Large copy number variations appear to be mostly confined to placental lineages (Zamani Esteki et al., 2019) due to developmental bottlenecks occurring during the first lineage segregation which genetically isolate TE from ICM (Coorens et al., 2021). Taken together, there is

ample evidence supporting the selective elimination of aneuploid cells from the embryonic lineage during pre- and post-implantation development, while the extraembryonic tissues appear to be more tolerant to genetic imbalances.

From a cellular point of view, aneuploidy has two types of consequences: a generic response and one that depends on the specific aneuploidy. The first type of response is highly conserved and has been found from yeast and plants to mouse and human cells (reviewed in: Santaguida and Amon, 2015; Zhu et al., 2018; Chunduri and Storchová, 2019; Chunduri et al., 2022; Krivega et al., 2022). Aneuploidy results in gene-dosage defects, leading to an unbalanced protein pool that induces the activation of the mechanisms to restore protein homeostasis, such as the chaperone system, the ubiquitin proteasome system and autophagy (Ariyoshi et al., 2016; Dürrbaum et al., 2014; Santaguida et al., 2015; Stingele et al., 2012). If these systems are overwhelmed, the accumulation of misfolded or aggregated proteins induces proteotoxic stress which is detrimental to the cells (Donnelly et al., 2014; Huettel et al., 2008; Ohashi et al., 2015; Oromendia et al., 2012; Stingele et al., 2012; Tang et al., 2011; Torres et al., 2007; Williams et al., 2008). Further, aneuploidy can cause replication stress, which in turn can lead to DNA-damage (Passerini et al., 2016; Santaguida et al., 2017; Sheltzer et al., 2011), p53 activation (Li et al., 2010; Santaguida et al., 2017; Thompson and Compton, 2010) and ultimately to cell cycle arrest and apoptosis (reviewed in: Santaguida and Amon, 2015; Zhu et al., 2018; Regin et al., 2022).

These mechanisms also appear to be active during early embryonic development and to have a lineage specific effect. In mice, clearance of aneuploid cells by apoptosis requires the activation of autophagy and p53 (Singla et al., 2020). Aneuploid cells are only being eliminated by apoptosis in the ICM (Bolton et al., 2016) and at similar rates in the EPI and the PrE (Singla et al., 2020). In a study using human 2D gastruloids with reversine-induced aneuploidy, apoptosis was only induced in differentiating but not in pluripotent cells, although aneuploidy did induce an increase in total nuclear p53 in both cell types. Similarly, as in the mouse, the aneuploid cells were eliminated by apoptosis from the embryonic germ layers but were tolerated in the TE-like cells (Yang et al., 2021).

The type of aneuploidy and the percentage of aneuploid cells within a euploid/aneuploid mosaic embryo determine its developmental capacity. The viability of mouse embryos inversely correlates to the proportion of aneuploid cells, with 50% of euploid cells being sufficient to sustain normal development (Bolton et al., 2016). This same threshold appears to apply to human embryos, where embryos with less than 50% of aneuploid cells have higher developmental potential than those containing more than 50%, albeit both performing worse than fully euploid embryos (Viotti et al., 2021, Capalbo et al., 2021).

Conversely, whole chromosome gains and losses that are present in every cell of the human embryo are usually linked to lethality with the notable exception of trisomies 13 (Patau syndrome), 18 (Edwards syndrome) and 21 (Down syndrome), and sex chromosome abnormalities. The effects of these imbalances can manifest already during early embryo development (Fuchs Weizman et al., 2019; Licciardi et al., 2018; Sanchez-Ribas et al., 2019; Shahbazi et al., 2020). Shahbazi *et al.* recently described the consequences of carrying specific meiotic aneuploidies on human embryo development using an in vitro implantation model (Shahbazi et al., 2020). They showed that human embryos with trisomy 15, 16 and 21 and monosomy 21 readily all reached the blastocyst stage, and that monosomy 21 embryos arrested after implantation while trisomy 15 and 21 embryos developed further. Interestingly, trisomy 16 embryos showed a hypoproliferative trophoblast due to excessive CDH1 expression, a gene located on chromosome 16.

In this study, we investigated the cellular responses to complex aneuploidy during human preimplantation development, with a focus on stress response and lineage segregation events. We assessed previously unexplored general consequences of naturally acquired aneuploidies in

human embryos with focus on impaired lineage segregation events.

Methods

Ethical approval

All experiments have been approved by the local Commission of Medical Ethics of the UZ Brussel (B.U.N. 143201628722) and the Federal Committee for Medical and Scientific Research on Human Embryos in vitro (AdV069 and AdV091). Patients from Brussels IVF (UZ Brussel) donated their embryos for research after written informed consent.

Culture of human pre-implantation embryos

All human embryos, unless stated otherwise, were warmed using the Vitrification Thaw Kit (Vit Kit-Thaw; Irvine Scientific, USA) and cultured in 25 µL droplets of Origio Sequential Blast^{TM} medium (Origio) at 37°C with 5% O_2, 6% CO_2 and 89% N_2. Embryos were graded before vitrification by experienced clinical embryologists according to Gardner and Schoolcraft criteria (Gardner and Schoolcraft, 1999).

Experiment 1

We warmed vitrified human blastocysts (5-6dpf) after PGT (28 euploid and 22 aneuploid) or at 3dpf (n=11). Post PGT-embryos were left to recover for 2h in culture medium, after which they underwent a second TE biopsy. For the reversine experiment, we cultured the 3dpf embryos for 24h in culture medium supplemented with 0.5 µM reversine (Stem Cell Technologies) and after wash-out we let them develop until 5dpf and subsequently took a biopsy. The concentration of 0.5 µM reversine was chosen based on previous experiments in mouse embryos (Bolton et al., 2016; Singla et al., 2020).

Experiment 2

We warmed 12 vitrified and undiagnosed human blastocysts (5-6dpf) of which 6 were cultured in culture medium for 16hrs. The other 6 embryos were cultured in medium supplemented with 0.1mg/mL Bleomycin (Sigma-Aldrich) for 16hrs.

Experiment 3

We warmed vitrified human blastocysts (5-6dpf) after PGT (7 euploid and 11 aneuploid) that were left to recover for 2hrs in culture medium.

Experiment 4

We warmed 5dpf-6dpf PGT embryos (10 euploid and 14 aneuploid) and cultured them for 16h to ensure sufficient time to progress to the second lineage differentiation. Prior to fixation we live-stained all the embryos with either Caspase-3/7 or Caspase-8 (Supplementary Table 9) for 30 min. Additionally, we warmed 5dpf-6dpf PGT embryos (6 euploid and 4 aneuploid) and cultured them for 16h without live-staining.

Biopsy procedure

The zona pellucida was opened (15-25µm) on 4dpf using a Saturn Laser (Cooper Surgical). For PGT cycles, expanded good quality embryos were biopsied on 5dpf; early blastocysts were evaluated again for expansion on 6dpf. Briefly, embryos were transferred to HEPES buffered medium and biopsied on a Nikon inversed microscope equipped with a Saturn Laser. The herniated TE cells were then aspirated and cut using manual laser shoots. In case of sticking cells this was supported

by mechanical cutting. After successful tubing, the blastocysts were vitrified using CBS-VIT High-Security straws (CryoBioSystem, L'Aigle, France) with dimethylsulphoxide-ethylene glycol-sucrose as the cryoprotectants (Irvine Scientific Freeze Kit, Newtownmountkennedy, County Wicklow, Ireland) (Van Landuyt et al., 2011). The TE biopsy for RNA-sequencing (Experiment 1) was performed with the same procedure, cells were biopsied from the same opening in the zona pellucida.

PGT

During PGT, our Center of Medical Genetics at the UZ Brussels analyzed a TE sample with multiple cells for each embryo. Next Generation Sequencing: The chromosomal analysis was performed by WGA (Sureplex, Illumina) followed by library preparation (KAPA HyperPlus, Roche), sequencing on a NovaSeq (Illumina) and an in-house developed interpretation pipeline. The analysis has an effective resolution of 5 Mb.

SNP-array

We relied on whole genome amplification (MDA, Repli-G) followed by genome wide SNP array using Karyomapping (Vitrolife) with Bluefuse software (Vitrolife). In addition, SNP array data were analyzed with an in-house developed interpretation pipeline for aneuploidy detection.

RNA-sequencing

Multiple (5-10) TE cells were used as input to generate full length cDNA with the SMART-SeqTM v4 UltraTM Low Input RNA Kit (Clontech Laboratories, Inc.) according to the manufacturer's instructions. The quality of cDNA was checked using the AATI Fragment Analyzer (Advances Analytical). Library preparation was performed using the KAPA HyperPlus Library Preparation Kit (KAPA Biosystems) according to the manufacturer's instructions. During cDNA synthesis and library preparation we used 17 and 11 PCR cycles, respectively. Sequencing was performed on a NovaSeq 6000 (Illumina) with 25 million reads per sample.

Bioinformatics analysis

Reads were trimmed using cutadapt version 1.11 to remove the "QuantSEQ FWD" adaptor sequence. We checked the quality of the reads using the FastQC algorithm (Love et al., 2014). Count tables were generated using STAR (Dobin et al., 2013) (version 2.5.3) through mapping against the Genome Reference Consortium Human Build 38 patch release 10 (GRCh38.p10) combined with a general transfer format (GTF) file, both downloaded from the Ensembl database. The RNA-sequencing by Expectation Maximization (RSEM) (Li and Dewey, 2011) software (version 1.3.0) was used to produce the count tables.

Differential gene expression analysis was performed using R-studio (Version 1.1.456) with the edgeR (Robinson et al., 2009) and limma (Ritchie et al., 2015) packages. We included genes with a count per million greater than 1 in at least two samples. The trimmed mean of M values (Robinson and Oshlack, 2010) algorithm was used for normalization. The normalized counts were then transformed in a $\log_2$ fold-change ($\log_2$FC) table with their associated statistics. In each comparison, genes with a $|\log_2 FC| > 1$ and an FDR < 0.05 were considered as significantly differentially expressed.

Gene set enrichment analysis (GSEA) was performed using the GSEA software (version 4.3.2) from the Molecular Signature Database (*https://www.gsea-msigdb.org/gsea/msigdb/index.jsp*). We generated a ranked gene list based on the normalized count matrix of the whole transcriptome that was detected after differential gene expression. The ranked gene list was then subjected to the GSEA function, and we searched the Hallmark and C2 library for significantly enriched pathways. Significance was determined using a cut-off value of 25% FDR. This cut-off is proposed in the user

guide of the GSEA (*https://www.gsea-msigdb.org/gsea/doc/GSEAUserGuideTEXT.htm*) especially for incoherent gene expression datasets, as suggested by our PCAs, which allows for hypothesis driven validation of the dataset.

The copy number variation (CNV) analysis was inferred from our RNA-sequencing data set using inferCNV R package (version 1.7.1) (Inferring copy number alterations from tumor single cell RNA-Seq data (*https://github.com/broadinstitute/inferCNV/wiki*"). Our count table was used as input and compared to the reference set which in our case was the expression data of the euploid embryos. The analysis followed the standard workflow in inferCNV with the following parameters: "denoise" mode, value of 1 was used for the "cutoff", prediction of CNV states using default Hidden Markov Models (HMM) method, "cluster_by_groups" was set to TRUE, and other values were set by default.

Gene dosage analysis

We calculated the total number of loci with imbalanced gene expression based on the genetic abnormalities identified during the PGT. For this, we used the number of coding loci per chromosomal region as listed in the ENSMBL database (*ensemble.org*) and included both gains and losses, either mosaic or homogeneously present, and both full chromosomal aneuploidy as well as segmental abnormalities. The embryos were ranked based on the total number of imbalanced loci and separated into a low- and a high-imbalanced gene dosage group. The low-dosage group contained the embryos with the lowest 50^{th} percentile in number of unbalanced loci, the high-dosage group the embryos with 50^{th} percentile or higher.

Immunocytochemistry

Prior to fixation we removed the zona pellucida using pre-warmed to 37°C Acidic Tyrode's Solution (Sigma-Aldrich) for 30 sec – 2 min and subsequently washed in PBS/2%BSA. Embryos were then fixed using 4% paraformaldehyde (Sigma-Aldrich) for 10 min, washed three times in PBS/2%BSA for 5 min and then permeabilized using 0.1% Triton X-100 (Sigma-Aldrich) for 20 min followed by another washing cycle. We used PBS/2% BSA supplemented with 10% FBS for 1h to block non-specific protein binding. The embryos were then incubated overnight with primary antibodies (Supplementary Table 9) diluted in blocking buffer at 4°C. The next day, they underwent another washing cycle using PBS/2%BSA and were then incubated with secondary antibodies (1:200, Supplementary Table 9) for 1h at room temperature. After washing, nuclei were stained using Hoechst 33342 (5µg/mL, Life Technologies) diluted in PBS/2%BSA for 15 min. For imaging we mounted the embryos on poly-L-lysine coated glass slides (Sigma-Aldrich) in 3µL of PBS. To avoid flattening of the embryos we used Secure-Seal^{TM} Spacers (9mm diameter, 0.12mm deep, Thermofisher) before putting the coverslips in place. For the experiments that required re-staining we imaged the embryos in 3µL PBS/2%BSA in 18 well µ-Slides (Ibidi) and subsequently recuperated them. After recuperation we photobleached the embryos stained for CASP3/7 by using maximum laser power of the 488 nm channel and maximum size of the pinhole for 10 min. The embryos were then re-stained using rat anti-GATA4 primary antibody and the matching Alexa Fluor 488 secondary antibody (Supplementary Table 9) (to replace the CASP3/7 staining).

Imaging and image analysis

Confocal imaging was performed using the LSM800 (Zeiss). Z-stacks were taken with a LD C-Apochromat 40x/1.1 NA water immersion objective in optical sections of 1µm. Nuclei were counted using the Blob finder function of Arivis Vision 4D (3.4.0). All other measurements were performed using the Zen 2 (blue edition) or Image J software based on the optical sections and/or orthogonal projections.

Statistics

The type of statistical test and p-values are mentioned in the figure legends. For most comparisons we used one-way ANOVA or Student's t-test with or without Welch's correction. For experiments that contained groups with small sample sizes we used non-parametric tests (Mann-Whitney). Fisher-exact test was used to determine the dependency of the ploidy status on the presence or absence of primitive endoderm. We used GraphPad Prism 9.0.0 for statistical testing. The trend analysis regarding gene dosage effects was performed with SPSS using the Jonckheere-Terpstra test.

Results

Human embryos with complex aneuploidy show gene dosage defects and transcriptomic signatures of p53 activation and apoptosis

We first tested for the presence of a common transcriptomic response to different complex aneuploidies. For this, we studied the transcriptome of a TE biopsy of fifty human blastocysts (5 or 6dpf) previously diagnosed by Preimplantation Genetic Testing (PGT) as either euploid or as containing an aneuploidy of at least two whole chromosomes in all cases except for one embryo (further referred to as aneuploid, detailed karyotypes can be found in the Supplementary Table 1). The aneuploidy was presumed to have occurred during meiosis or during the first cleavage from zygote to the 2-cell stage, resulting in all or most of the cells of the TE biopsy containing the same genetic imbalances. We also included a TE sample of eleven human blastocysts that were treated with 0.5 μM reversine from 3dpf to 4dpf, to induce complex mosaic aneuploidy (referred to as reversine-treated embryos). Of these, 14 euploid, 20 aneuploid and 11 reversine-treated embryos yielded good quality RNA-sequencing results.

Principal component analysis using all expressed genes revealed no clustering of the euploid, aneuploid or reversine-treated embryos into distinct groups (**Fig. 1a**, **Supplementary Figure 1a**). We used InferCNV (*https://github.com/broadinstitute/inferCNV/wiki*) to bioinformatically infer the chromosomal copy numbers based on the higher or lower expression of the genes located on chromosomes with gains or losses (**Fig. 1b**, **Supplementary Fig. 1b,c**). We compared the inferred karyotypes to those obtained during PGT and found a match for 45/48 of the full chromosome aneuploidies, while euploidy was correctly predicted in all cases (**Supplementary Fig. 1b**). These results show that aneuploidy in human blastocysts results in abnormal gene dosage effects. Of note, the karyotypes of the reversine-treated embryos could not be determined since this drug induces different aneuploidies in each cell, leading to mosaic TE biopsies. Also, the karyotypes of the 3dpf embryos were not determined by PGT before the reversine treatment. InferCNV detected only a trisomy 12 in one of the reversine-treated embryos, likely of meiotic or first-cleavage origin (**Supplementary Figure 1c**).

Despite the abnormal gene dosage, but in line with the lack of clear clustering in the PCA, the differential gene expression analysis yielded 21 significantly upregulated and 2 downregulated genes (**Fig. 1c**, Supplementary Table 2). These findings are similar to those of other studies on the transcriptome of aneuploid human embryonic cells, which also found a few significantly deregulated genes (Fernandez Gallardo et al., 2023; Groff et al., 2019; Martin et al., 2023; Maxwell et al., 2022). We next focused on pathway analysis based on a ranked gene list of the whole transcriptome. We found that cellular stress gene sets were positively enriched in the aneuploid samples, including the p53-pathway and apoptosis (**Fig. 1d-f**). Gene sets related to metabolism, translation, mitochondrial function and proliferation, such as translation and ribosome, oxidative phosphorylation and MYC targets, were negatively enriched (**Fig. 1d-f**).

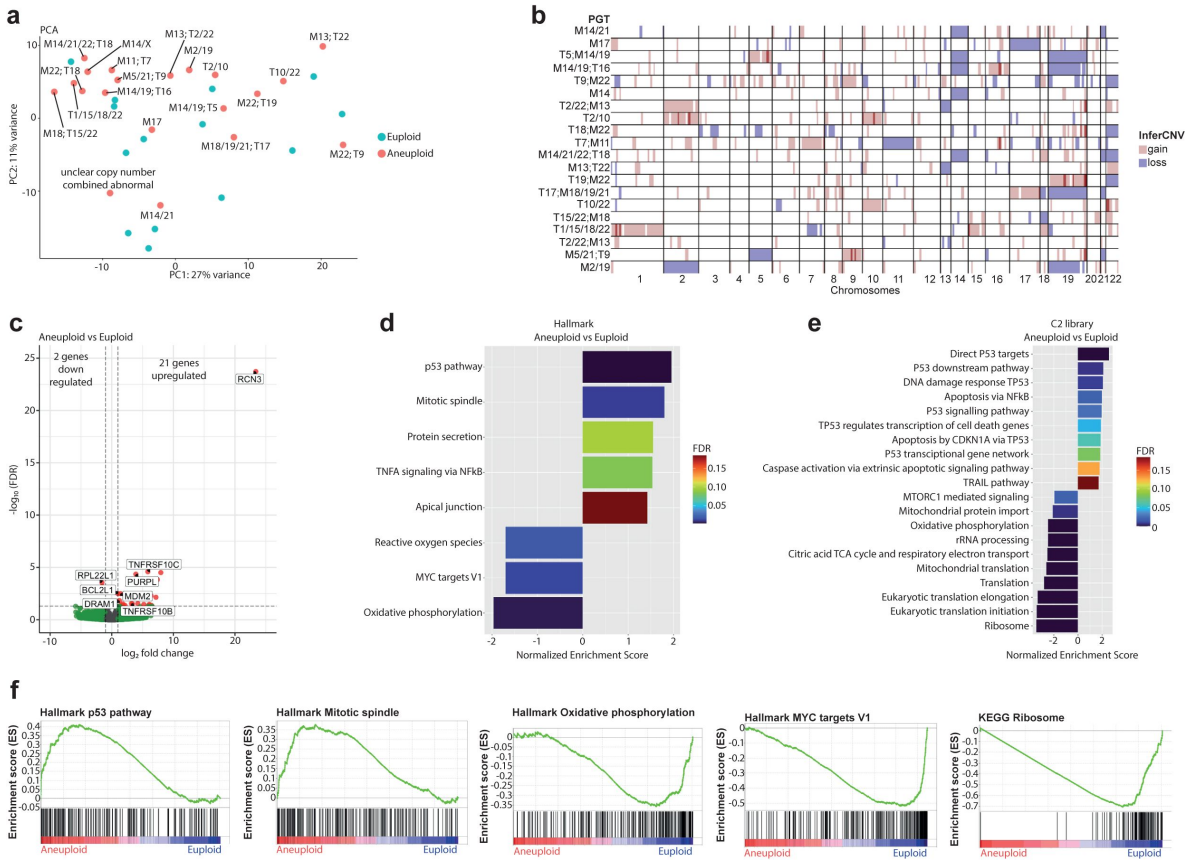

Fig. 1

RNA-sequencing of trophectoderm cells reveals gene dosage defects and transcriptomic signatures of p53 activation and apoptosis

a. Principal component analysis after transcriptome analysis of aneuploid versus euploid embryos. T= Trisomy, M=Monosomy. **b**. Comparison between the diagnosis of aneuploid embryos obtained after PGT (list on the left) and the results obtained after using InferCNV after RNA-sequencing (plot on the right). Red and blue indicate gain or loss of the chromosome, respectively. **c**. Volcano plot after differential gene expression analysis with a cutoff value of $|\log_2$ fold change$| > 1$ and $-\log_{10}(\text{FDR}) < 0.05$ for aneuploid versus euploid embryos showing 21 upregulated and 2 downregulated genes. **d.** Barplot of enriched Hallmark pathways after gene set enrichment analysis of aneuploid versus euploid embryos using a cut-off value of 25% FDR. **e.** Barplot of TOP20 enriched C2 library pathways after gene set enrichment analysis of aneuploid versus euploid embryos using a cut-off value of 25% FDR. **f.** Enrichment plots of p53-pathway, mitotic spindle, oxidative phosphorylation, MYC targets V1 and ribosome, showing up- or downregulation of genes that are part of the corresponding pathway. Source of all embryos: Experiment 1.

When comparing reversine-treated versus euploid embryos we found 34 significantly upregulated and 22 significantly downregulated genes (**Supplementary Fig 1d-f**, Supplementary Table 3). The expression profile differed from that identified in the endogenously aneuploid embryos. Here, we found mitotic spindle, WNT-beta catenin signalling, KRAS signalling and lysosome gene sets to be positively enriched while oxidative phosphorylation, MYC targets, translation and ribosome were negatively enriched. We found no evidence for p53 activation or apoptosis. This suggests that naturally acquired aneuploidies of meiotic origin may elicit a different transcriptomic response than reversine-induced mitotic aneuploidies, with a differential induction of the p53 signalling pathway and apoptosis, and inhibition of proliferation.

High gene-dosage imbalances result in high p53 activation and apoptosis while low gene dosage imbalances induce pro-survival pathways

To test whether there is a relationship between the type of cellular stress signatures and the size of the chromosomal imbalances, as previously described in cancer cells (Dürrbaum and Storchová, 2016), we categorized the aneuploid embryos into a low- and a high-imbalanced gene dosage group. This separation was based on the total number of coding loci that were affected by the aneuploidies (Supplementary Table 4). The low-dosage group contained the embryos under the 50^{th} percentile when ranking the embryos from the lowest to the highest number of unbalanced loci. The high-dosage group contained the embryos with 50^{th} percentile or higher. Principal component analysis showed that high-dosage embryos clustered separately from the euploid embryos (**Fig. 2a**), with 65 significantly upregulated and 153 significantly downregulated genes (**Fig. 2b**, Supplementary Table 5). High dosage embryos showed a transcriptomic profile consistent with activation of the p53-pathway and apoptosis, while the unfolded protein response, DNA-repair, MYC targets, oxidative phosphorylation, translation and ribosome were inhibited (**Fig. 2c-e**).

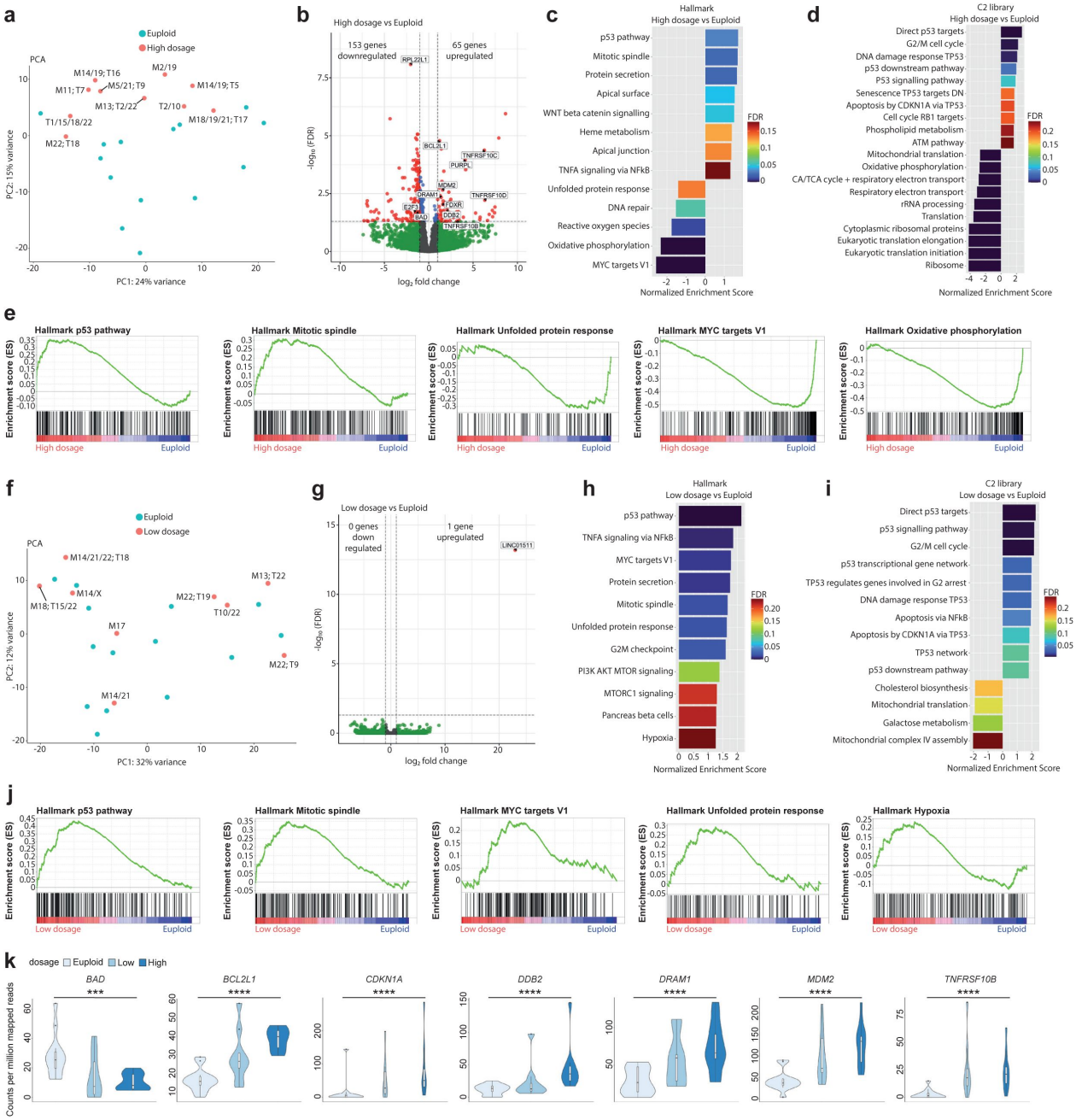
a
Euploid
High dosage
PCA
PC2: 15% variance
PC1: 24% variance
b
High dosage vs Euploid
153 genes downregulated
65 genes upregulated
log2 fold change
c
Hallmark
High dosage vs Euploid
p53 pathway
Mitotic spindle
Protein secretion
Apical surface
WNT beta catenin signalling
Heme metabolism
Apical junction
TNFA signaling via NFkB
Unfolded protein response
DNA repair
Reactive oxygen species
Oxidative phosphorylation
MYC targets V1
FDR
Normalized Enrichment Score
d
C2 library
High dosage vs Euploid
Direct p53 targets
G2/M cell cycle
DNA damage response TP53
p53 downstream pathway
P53 signalling pathway
Senescence TP53 targets DN
Apoptosis by CDKN1A via TP53
Cell cycle RB1 targets
Phospholipid metabolism
ATM pathway
Mitochondrial translation
Oxidative phosphorylation
CA/TCA cycle + respiratory electron transport
Respiratory electron transport
rRNA processing
Translation
Cytoplasmic ribosomal proteins
Eukaryotic translation elongation
Eukaryotic translation initiation
Ribosome
FDR
Normalized Enrichment Score
e
Hallmark p53 pathway
Hallmark Mitotic spindle
Hallmark Unfolded protein response
Hallmark MYC targets V1
Hallmark Oxidative phosphorylation
Enrichment score (ES)
High dosage
Euploid
f
Euploid
Low dosage
PCA
PC2: 12% variance
PC1: 32% variance
g
Low dosage vs Euploid
0 genes down regulated
1 gene upregulated
log2 fold change
h
Hallmark
Low dosage vs Euploid
p53 pathway
TNFA signaling via NFkB
MYC targets V1
Protein secretion
Mitotic spindle
Unfolded protein response
G2M checkpoint
PI3K AKT MTOR signaling
MTORC1 signaling
Pancreas beta cells
Hypoxia
FDR
Normalized Enrichment Score
i
C2 library
Low dosage vs Euploid
Direct p53 targets
p53 signalling pathway
G2/M cell cycle
p53 transcriptional gene network
TP53 regulates genes involved in G2 arrest
DNA damage response TP53
Apoptosis via NFkB
Apoptosis by CDKN1A via TP53
TP53 network
p53 downstream pathway
Cholesterol biosynthesis
Mitochondrial translation
Galactose metabolism
Mitochondrial complex IV assembly
FDR
Normalized Enrichment Score
j
Hallmark p53 pathway
Hallmark Mitotic spindle
Hallmark MYC targets V1
Hallmark Unfolded protein response
Hallmark Hypoxia
Enrichment score (ES)
Low dosage
Euploid
k
dosage Euploid Low High
BAD
BCL2L1
CDKN1A
DDB2
DRAM1
MDM2
TNFRSF10B
Counts per million mapped reads

Fig. 2

Human embryos with the highest number of genes with abnormal copy number show stronger p53 pathway and apoptosis response.

a. Principal component analysis after transcriptome analysis of high-dosage aneuploid versus euploid embryos. T= Trisomy, M=Monosomy. **b**. Volcano plot after differential gene expression analysis with a cutoff value of $|\log_2$ fold change$|$ > 1 and $-\log_{10}$(FDR) < 0.05 for high-dosage aneuploid versus euploid embryos showing 65 upregulated and 153 downregulated genes. **c.** Barplot of enriched Hallmark pathways after gene set enrichment analysis of high-dosage aneuploid versus euploid embryos using a cut-off value of 25% FDR. **d.** Barplot of TOP20 enriched C2 library pathways after gene set enrichment analysis of high-dosage aneuploid versus euploid embryos using a cut-off value of 25% FDR. **e.** Enrichment plots of p53-pathway, mitotic spindle, unfolded protein response, MYC targets V1 and oxidative phosphorlation, showing up- or downregulation of genes that are part of the corresponding pathway. **f**. Principal component analysis after transcriptome analysis of low-dosage aneuploid versus euploid embryos. T= Trisomy, M=Monosomy. **g**. Volcano plot after differential gene expression analysis with a cutoff value of $|\log_2$ fold change$|$ > 1 and $-\log_{10}$(FDR) < 0.05 for low-dosage aneuploid versus euploid embryos showing 1 upregulated and 0 downregulated genes. **h.** Barplot of enriched Hallmark pathways after gene set enrichment analysis of low-dosage aneuploid versus euploid embryos using a cut-off value of 25% FDR. **i.** Barplot of enriched C2 library pathways after gene set enrichment analysis of low-dosage aneuploid versus euploid embryos using a cut-off value of 25% FDR. **j.** Enrichment plots of p53-pathway, mitotic spindle, MYC targets V1, unfolded protein response and hypoxia showing upregulation of genes that are part of the corresponding pathway. **k.** Violin plots with box and whisker plots of the counts per million mapped reads of a supervised set of 10 that are part of apoptosis (*BAD, BCL2L1, TNFRSF10B*), p53 pathway (*DRAM1, MDM2, CDKN1A*), and DNA-damage (*DDB2*). *p = 0.027, **p = 0.010, ***p = 0.004, ****p < 0.001 using the Jonkheere-Terpstra test. Box and whisker plots show median and minimum to maximum values. Source of all embryos: Experiment 1.

In contrast, low-dosage embryos lacked separation from the euploid embryos in the PCA (**Fig. 2f**) and only had one differentially expressed gene (**Fig. 2g**). While we still found aneuploidy related stress responses such as p53-pathway and apoptosis to be activated, we found also pro-survival gene sets such as MYC targets (Dang et al., 2006; Wang et al., 2021), MTORC1 signalling (Hung et al., 2012), unfolded protein response (Hetz et al., 2020; Zanetti et al., 2016) and hypoxia (Simões-Sousa et al., 2018) to be enriched (**Fig. 2h-j**). Low-dosage embryos showed no profiles of ribosome or translation impairment. Last, the plotting of the expression levels of genes in the p53 and apoptosis pathways show their progressive stronger induction or suppression from euploid to low and high dosage embryos (**Fig. 2k**). This illustrates the association between the severity of the protein pool imbalance and the induction of the cellular stress response.

Aneuploidy triggers proteotoxic stress, DNA-damage independent p53-activation, autophagy and apoptosis

To further investigate the cellular stress responses identified by the transcriptomic analysis, we carried out immunostaining on the same embryos that underwent TE biopsy for transcriptome analysis. The results show that aneuploid and reversine-treated embryos have increased signal intensity of active CASP3/7 and CASP8 (**Fig. 3a-d**). Both aneuploid and reversine-treated embryos also have lower cell numbers than euploid embryos, likely due to the apoptosis-mediated cell loss (**Fig. 3e**).

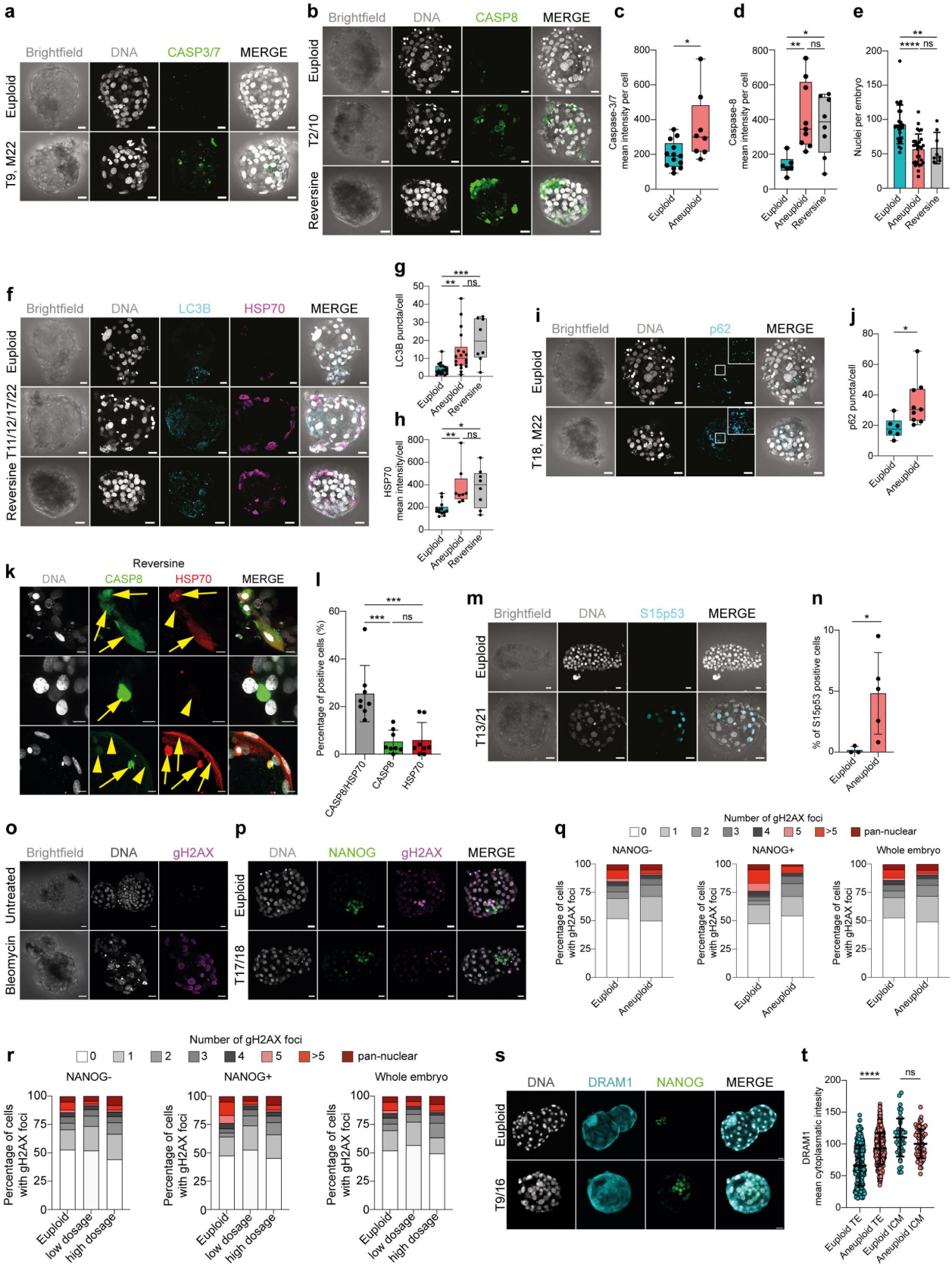
a
Brightfield
DNA
CASP3/7
MERGE
Euploid
T9, M22
b
Brightfield
DNA
CASP8
MERGE
Euploid
T2/10
Reversine
c
Caspase-3/7 mean intensity per cell
Euploid
Aneuploid
d
Caspase-8 mean intensity per cell
Euploid
Aneuploid
Reversine
e
Nuclei per embryo
Euploid
Aneuploid
Reversine
f
Brightfield
DNA
LC3B
HSP70
MERGE
Euploid
Reversine T11/12/17/22
g
LC3B puncta/cell
h
HSP70 mean intensity/cell
i
Brightfield
DNA
p62
MERGE
Euploid
T18, M22
j
p62 puncta/cell
k
Reversine
DNA
CASP8
HSP70
MERGE
l
Percentage of positive cells (%)
CASP8/HSP70
CASP8
HSP70
m
Brightfield
DNA
S15p53
MERGE
Euploid
T13/21
n
% of S15p53 positive cells
o
Brightfield
DNA
gH2AX
Untreated
Bleomycin
p
DNA
NANOG
gH2AX
MERGE
Euploid
T17/18
q
Number of gH2AX foci
0
1
2
3
4
5
>5
pan-nuclear
NANOG-
NANOG+
Whole embryo
Percentage of cells with gH2AX foci
r
Number of gH2AX foci
NANOG-
NANOG+
Whole embryo
Euploid
low dosage
high dosage
s
DNA
DRAM1
NANOG
MERGE
Euploid
T9/16
t
DRAM1 mean cytoplasmatic intensity
Euploid TE
Aneuploid TE
Euploid ICM
Aneuploid ICM

Fig. 3

Immunostaining reveals increased proteotoxic stress, DNA-damage independent p53-activation, autophagy and apoptosis

a. Orthogonal projections after immunostaining of euploid and aneuploid embryos for DNA (white) and CASP3/7 (green). T= Trisomy, M=Monosomy. Source: Experiment 1. **b.** Orthogonal projections after immunostaining of euploid, aneuploid and reversine-treated embryos for DNA (white) and CASP8 (green). T= Trisomy. Source: Experiment 1. **c**. CASP3/7 mean intensity per cell. Euploid n=13, Aneuploid n=8 embryos. Unpaired t-test, *p = 0.0177. Source: Experiment 1. **d**. CASP8 mean intensity per cell. Euploid n=6, Aneuploid n=9, Reversine-treated n=8 embryos. One-way ANOVA, *p = 0.04, **p = 0.0098, ns= non-significant. Source: Experiment 1. **e**. Number of nuclei per embryo. Euploid n=26, Aneuploid n=29, Reversine-treated n=8 embryos. One-way ANOVA, ****p < 0.0001, **p = 0.0033, ns= non-significant. Source: Experiment 1 and 3. **f.** Orthogonal projections after immunostaining of euploid, aneuploid and reversine-treated embryos for DNA (white), LC3B (turquoise) and HSP70 (magenta). T= Trisomy. Source: Experiment 1. **g.** LC3B puncta per cell. Euploid n=19, Aneuploid n=22 embryos, Reversine-treated n=8 embryos. One-way ANOVA, **p = 0.0069, ***p = 0.0003, ns= non-significant. Source: Experiment 1. **h**. HSP70 mean intensity per cell. Euploid n=13, Aneuploid n=8, Reversine-treated n=8 embryos. One-way ANOVA, *p = 0.0121, **p = 0.0096, ns= non-significant. Source: Experiment 1. **i**. Orthogonal projections after immunostaining of euploid, aneuploid for DNA (white) and p62 (turquoise). White square shows zoom of a representative area. T= Trisomy, M=Monosomy. Source: Experiment 1. **j.** p62 puncta per cell. Euploid n=6, Aneuploid n=9 embryos. Unpaired t-test, *p = 0.0284. Source: Experiment 1. **k.** Optical sections of reversine treated embryos for DNA (white), CASP8 (green), HSP70 (red) showing cells with presence (yellow arrow) or absence (yellow arrowhead) of the proteins to investigate co-localization. Source: Experiment 1. **l.** Percentage of cells of reversine embryos positive for either CASP8/HSP70, CASP8 or HSP70. One-way ANOVA, CASP8/HSP70 vs CASP8***p = 0.0003, CASP8/HSP70 vs HSP70***p = 0.0005, ns= non-significant. Source: Experiment 1. **m.** Orthogonal projections after immunostaining of euploid, aneuploid for DNA (white) and Serine (S) 15 p53 (turquoise). Source: Experiment 4. **n.** Percentage of Serine 15 p53 positive cells per embryo. Euploid n = 3, Aneuploid n = 5. Unpaired t-test with Welch's correction, *p = 0.0356. T= Trisomy. Source: Experiment 4. **o.** Orthogonal projections of immunostained untreated (n = 6) and Bleomycin treated (n = 6) embryos for DNA (white) and gH2AX (magenta) showing few foci in the untreated and pan-nuclear expression of gH2AX. Source: Experiment: 2. **p.** Orthogonal projections of immunostained euploid (n = 7) and aneuploid (n = 11) embryos for DNA (white), NANOG (green) and gH2AX (magenta). T= Trisomy. Source: Experiment 3. **q.** Percentage of cells with gH2AX foci or pan nuclear expression of euploid (n = 7) and aneuploid (n = 11) embryos in NANOG-negative, NANOG positive cells and whole embryos. Source: Experiment 3. **r.** Percentage of cells with gH2AX foci or pan nuclear expression of euploid (n = 7), low-dosage (n = 5) and high dosage (n = 6) aneuploid embryos in NANOG-negative, NANOG positive cells and whole embryos. Source: Experiment 3. **s.** Orthogonal projections of immunostained euploid (n = 6) and aneuploid (n = 11) embryos for DNA (white), DRAM1 (turquoise) and NANOG (green). T= Trisomy. Source: Experiment 3. **t.** DRAM1 mean cytoplasmatic intensity in TE and ICM of euploid and aneuploid cells. Euploid TE (n = 312 cells). Aneuploid TE (n = 434 cells). Euploid ICM (n = 43 cells). Aneuploid ICM (n = 70 cells). Each dot represents the cytoplasm of a single cell. One-way ANOVA, ****p<0.0001, ns = non-significant. Source: Experiment 3.

Embryo sources are indicated in each section. Brightfield pictures were obtained during confocal imaging. All scale bars are 20 µm. Box and whisker plots show median, and whiskers show minimum to maximum values. Bar plots and scatter plots show mean ± s.d.

We next sought to corroborate the transcriptomic signatures of proteotoxic stress and autophagy. The number of puncta per cell of LC3B, and p62, as well as the intensity of HSP70 staining, as markers of autophagy and chronic protein misfolding, were significantly increased in both aneuploid and reversine-treated embryos (**Fig. 3f-j**). We also tested for the colocalization of CASP8 and HSP70 at the individual cell level. We found that reversine-treated embryonic cells mainly co-express CASP8/HSP70, while the minority is single positive for either CASP8 or HSP70

(**Figure 3k,l**). These results show that although the transcriptomic profile of naturally occurring aneuploidies and reversine-treated embryos is moderately different (**Figure 1c-f**, **Supplementary Figure 1d-f**), the downstream protein response is similar.

One of the key activated pathways identified during the transcriptome analysis was p53-signalling. Thus, we sought to validate p53 activation by staining for the phosphorylation of Serine-15 on p53, which is phosphorylated upon stimuli such as DNA-damage and metabolic stress (Loughery et al., 2014). We found that indeed aneuploid embryos showed a higher percentage of cells with activated p53 (**Fig. 3m,n**). These differences did not reach significance when considering the ICM/EPI-OCT4-positive cells or TE OCT4-negative cells separately (**Supplementary Fig. 2a-c**) probably due to insufficient statistical power.

We then stained an additional batch of embryos (Supplementary Table 6) for the double-strand break marker gH2AX, with the aim of determining if the p53 activation was DNA-damage mediated. As a control, we treated human embryos with the DNA-damage inducer Bleomycin and compared them to untreated embryos. All cells of Bleomycin treated embryos showed a pan-nuclear gH2AX pattern, while untreated embryos rarely showed cells containing foci (**Fig. 3o**). Euploid and aneuploid embryos showed similar fractions of cells with gH2AX foci or pan-nuclear staining (**Fig. 3p,q**), which did not change when dividing the aneuploid embryos into high and low dosage groups, (**Fig. 3r**).

Lastly, the transcriptome analysis showed significant upregulation in aneuploid and high-dosage aneuploid embryos of the gene *DRAM1* (DNA Damage Regulated Autophagy Modulator-1, **Figure 2b**). DRAM1 is in the lysosomal membrane, and it increases autophagic flux and apoptosis after stress-induced p53 activation in cancer cells (Crighton et al., 2006; Guan et al., 2015). We stained euploid and aneuploid embryos (Supplementary Table 6) for DRAM1 and NANOG and found that the expression of DRAM1 is increased specifically in the cytoplasm of aneuploid TE cells but not in the ICM (NANOG-positive cells, **Figure 3s,t**).

Aneuploidy increases apoptosis in the trophectoderm and impairs lineage segregation events

We next investigated whether the stress responses to aneuploidy are cell-type specific, as shown in the mouse (Bolton et al., 2016; Singla et al., 2020) and human 2D gastruloids (Yang et al., 2021). Concretely, we aimed to study the consequences of aneuploidy during the first lineage segregation event to TE and ICM, and the second lineage segregation event to EPI and PrE.

We first immunostained euploid and aneuploid 5-6dpf human embryos for the pluripotency marker NANOG (Supplementary Table 6). NANOG protein was enriched in the nuclei of aneuploid TE and ICM cells (**Fig. 4a,b**), which could suggest a delay in the exit from pluripotency in both lineages. We then co-stained 6-7dpf euploid and aneuploid blastocysts for OCT4, CASP3/7 and LC3B (Supplementary Table 7). Overall, we found lower cell counts in both the TE (OCT-negative cells) and in the OCT4-positive cells (ICM/EPI cells), **Fig. 4c-e**) of aneuploid embryos. This resulted in lower total cell numbers in aneuploid embryos (**Fig. 4f**), in line with our previous observation (**Fig. 3e**). We found a higher percentage of nuclear CASP3/7 positive cells (**Fig. 4g,h**) as well as a higher CASP3/7 mean intensity per cell (**Fig. 4g,i**) specifically in the TE of aneuploid embryos. In contrast, not a single OCT4-positive cell of either the euploid or aneuploid embryos showed nuclear CASP3/7 signal (**Fig. 4g**). Aneuploid embryos also showed a higher number of CASP3/7-positive micronuclei in the cells (**Fig. 4j,k**). The lineage-specific response to aneuploidy also extended to presence of autophagy. The staining for LC3B showed that aneuploid embryos displayed overall increased levels of autophagy which was mainly taking place in the TE and not the ICM (**Fig. 4l-o**).

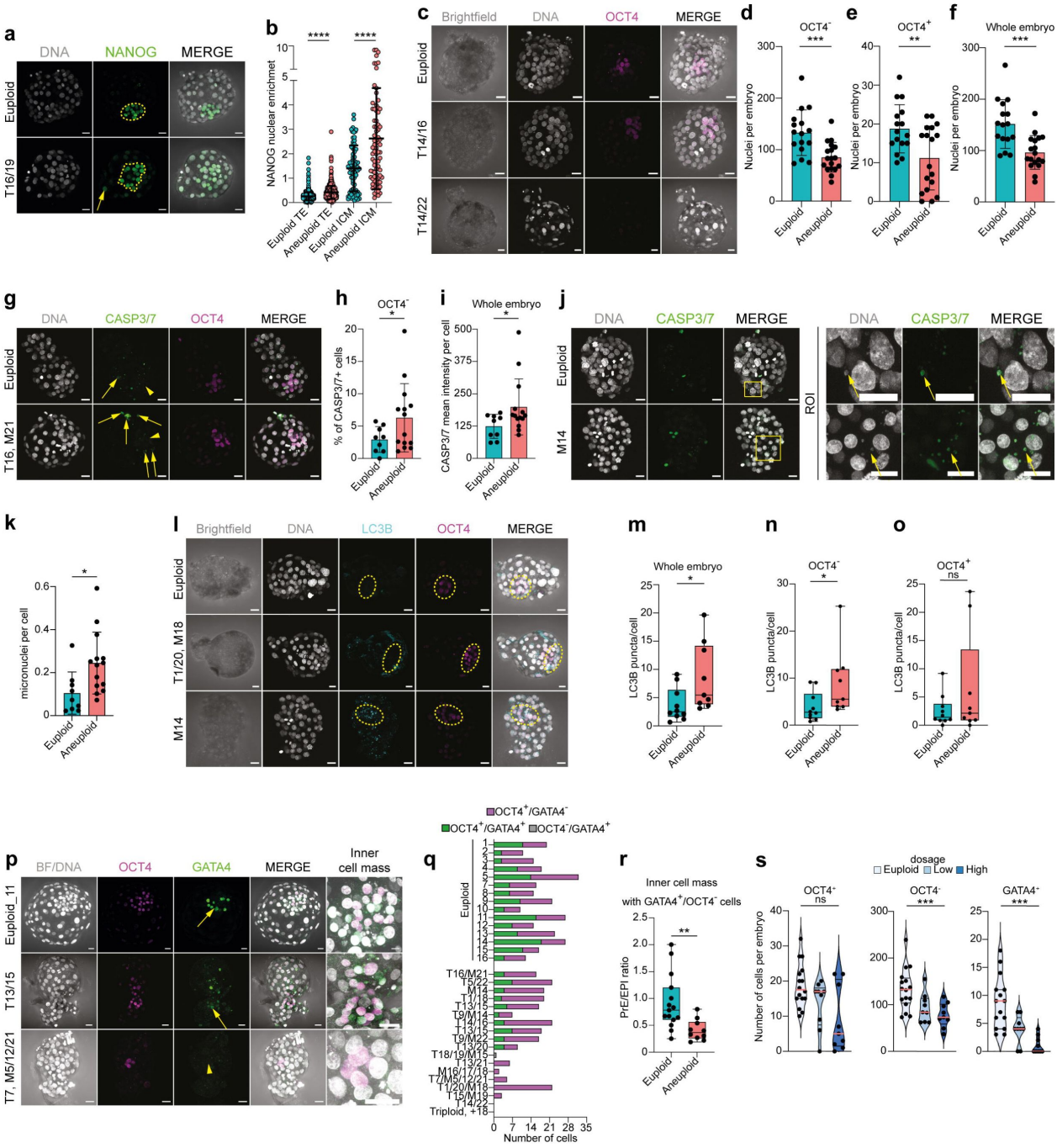
a
DNA
NANOG
MERGE
Euploid
T16/19
b
NANOG nuclear enrichmet
****
****
Euploid TE
Aneuploid TE
Euploid ICM
Aneuploid ICM
c
Brightfield
DNA
OCT4
MERGE
Euploid
T14/16
T14/22
d
OCT4⁻
***
Nuclei per embryo
Euploid
Aneuploid
e
OCT4⁺
**
f
Whole embryo
***
g
DNA
CASP3/7
OCT4
MERGE
Euploid
T16, M21
h
OCT4⁻
*
% of CASP3/7+ cells
i
Whole embryo
*
CASP3/7 mean intensity per cell
j
DNA
CASP3/7
MERGE
Euploid
M14
ROI
k
*
micronuclei per cell
l
Brightfield
DNA
LC3B
OCT4
MERGE
Euploid
T1/20, M18
M14
m
Whole embryo
*
LC3B puncta/cell
n
OCT4⁻
*
o
OCT4⁺
ns
p
BF/DNA
OCT4
GATA4
MERGE
Inner cell mass
Euploid_11
T13/15
T7, M5/12/21
q
OCT4⁺/GATA4⁻
OCT4⁺/GATA4⁺
OCT4⁻/GATA4⁺
Euploid
T16/M21
T5/22
M14
T1/18
T13/15
T9/M14
T14/16
T13/15
T9/M22
T13/20
T18/19/M15
T13/21
M16/17/16
T7/M5/12/21
T1/20/M18
T15/M19
T14/22
Triploid, +18
Number of cells
r
Inner cell mass
with GATA4⁺/OCT4⁻ cells
**
PrE/EPI ratio
s
dosage
Euploid
Low
High
OCT4⁺
ns
OCT4⁻
***
GATA4⁻
***
Number of cells per embryo

Fig. 4

Aneuploid human embryos show less cells in trophectoderm and OCT4-positive cells and impaired lineage segregation events

a. Orthogonal projections after immunostaining of euploid (n = 7) and aneuploid embryos (n = 10) for DNA (white) and NANOG (green). T= Trisomy. Source: Experiment 3. **b.** NANOG nuclear enrichment in cells of the TE and ICM of euploid and aneuploid embryos. Each dot represents the nucleus of a single cell. Euploid TE (n = 718 cells). Aneuploid TE (n = 708 cells). Euploid ICM (n = 77 cells). Aneuploid ICM (n = 77 cells). **c.** Orthogonal projections after immunostaining of euploid and aneuploid embryos for DNA (white) and OCT4 (magenta). The first aneuploid panel (Trisomy 14 and 16) shows a similar number of ICM cells compared to the euploid embryo. The second aneuploid panel (Trisomy 14 and 22) shows an embryo without an ICM. T= Trisomy. Source: Experiment 4. **d,e**,**f**. Differences in number of nuclei per embryo between euploid and aneuploid embryos in the (**d**) OCT4-negative cells (trophectoderm) ***p = 0.0006, (**e**) OCT4-positive cells (ICM/EPI), **p = 0.0055 and (**f**) whole embryo ***p = 0.0003. Euploid n = 16, Aneuploid n = 18. Unpaired t-test. Source: Experiment 4. **g.** Orthogonal projections after immunostaining of euploid and aneuploid embryos for DNA (white), CASP3/7 (green) and OCT4 (magenta). c. T= Trisomy, M= Monosomy. Yellow arrows indicate presence of the signal and yellow arrow heads indicate absence of signal. **h.** Percentage (%) of CASP3/7 positive (+) cells in the trophectoderm lineage (OCT4-negative cells). Euploid n = 9, Aneuploid n = 14. Unpaired t-test with Welch's correction, *p = 0.0453. Source: Experiment 4. **i**. CASP3/7 mean intensity per cell of whole embryos. Euploid n = 9, Aneuploid n = 14. Unpaired t-test with Welch's correction, *p = 0.0332. Source: Experiment 4. **j.** Left panel: Orthogonal projections after immunostaining of euploid and aneuploid embryos for DNA (white) and CASP3/7 (green) showing micronuclei. Yellow box indicates zoomed-in region of interest (ROI). Yellow arrows indicate presence of micronuclei and overlap between DNA and CASP3/7. Source: Experiment 4. **k**, Number of micronuclei per cell in euploid and aneuploid whole embryos. Euploid n = 9, Aneuploid n = 14. Unpaired t-test with Welch's correction, *p = 0.0115. Source: Experiment 4. **l**. Orthogonal projections after immunostaining of euploid and aneuploid embryos for DNA (white), LC3B (turquoise) and OCT4 (magenta). Yellow circle indicates the ICM. The first aneuploid panel (Trisomy 1 and 20 and monosomy 18) shows OCT4-positive cells (ICM/EPI) with low levels of autophagy. The second aneuploid panel (Monosomy 14) shows an embryo with high levels of autophagy in the ICM. Source: Experiment 4. **m,n,o.** Differences in LC3B puncta per cell between euploid (n=10) and aneuploid (n=9) embryos in the (**m**) whole embryo, *p = 0.0220, (**n**) OCT4-negative cells (trophectoderm),*p = 0.0172 and (**o**) OCT4-positive cells (ICM/EPI) ns = non-significant. Mann-Whitney test. Source: Experiment 4. **p.** Orthogonal projections after immunostaining of euploid and aneuploid embryos for DNA (white), OCT4 (magenta) and GATA4 (green). The first aneuploid panel (trisomy 13 and 15) shows an embryo with presence of GATA4 positive cellc (PrE). The second aneuploid panel (Trisomy 7 and monosomies 5, 12 and 21) shows an embryo that did not contain GATA4 positive cells. Source: Experiment 4. **q.** Differences in the number of cells per embryo that were OCT4 positive and either GATA4 negative (magenta) or positive (green) or OCT4 negative and GATA4 positive (grey) between euploid (n=15) and aneuploid (n=18) embryos. In case GATA4-positive cells (PrE) were present we considered the GATA4-negative cells to be epiblast (EPI). All euploid embryos contained GATA4-positive cells, 7/18 aneuploid embryos had an ICM completely lacking GATA4-positive cells (Fisher-exact test, p = 0.009). **r**, Differences in the PrE/EPI ratio between euploid and aneuploid embryos that had an ICM containing GATA4-positive cells. Euploid n = 15, Aneuploid n = 10. Unpaired t-test, **p = 0.0068. Source: Experiment 4. **s.** Violin plots with box plots of OCT4-positive-cells (ICM/EPI) per embryo (left, ns), OCT4-negative cells (trophectoderm) per embryo (center, ***p < 0.001) and GATA4-positive-cells (PrE) per embryo (right, ***p < 0.001, Jonkheere-Terpstra test) depending on gene dosage. Euploid (light blue), Low dosage (middle blue) and High dosage (darkest blue). Source: Experiment 4.

Brightfield pictures were obtained during confocal imaging. All scale bars are 20 µm. Box and whisker plots show median and minimum to maximum values. Bar plots show mean ± s.d. Besides (**b**) all dots represent one embryo.

Finally, we observed that the counts of OCT4-positive cells in the aneuploid embryos distributed in two groups: one with very low counts and one with counts in the range of that of euploid embryos (**Fig. 4e**). This led us to hypothesize that some of the aneuploid embryos had a delayed ICM development, with impairment of the second lineage segregation event. All blastocysts analyzed

above were re-stained for GATA4 (PrE marker) and imaged together with OCT4 (ICM/EPI marker). We found that while all euploid embryos contained GATA4-positive cells, 39% of aneuploid embryos had no GATA4-positive cells (**Fig. 4p,q**). Furthermore, in those aneuploid embryos that contained GATA4-positive PrE cells, there was a significantly lower ratio of GATA4-positive to OCT4-positive/GATA4-negative cells (**Fig. 4r**). Categorization of the aneuploid embryos into a low- and a high-dosage group (Supplementary Table 8) showed that the higher the number of imbalanced loci, the lower the cell numbers in the TE and PrE but not in the EPI (**Fig. 4s**).

Taken together, these results suggest that there are important differences in how the embryonic lineages respond to aneuploidy. While the TE is activating autophagy and apoptosis, this is not the case for the ICM/EPI. In turn, while in both lineages, aneuploidy appears to promote a delay in the downregulation of NANOG during differentiation, the ICM of high-dosage aneuploid embryos frequently has poor or no differentiation to PrE.

Discussion

In this work, we studied the consequences of uniform complex aneuploidy in human preimplantation embryos. In our study we find that, while aneuploid embryos had lower cell numbers in both TE and ICM/EPI, the effect of aneuploidy was cell-type dependent. Aneuploid TE presented transcriptomic signatures of p53 signalling and apoptosis, and immunostaining of whole embryos showed that aneuploidy results in increased proteotoxic stress, autophagy, activated p53 independent from DNA-damage and subsequent apoptosis. In contrast, in the ICM, aneuploidy affects PrE formation.

Overall, our gene-expression results are in line with previously published RNA-sequencing studies on aneuploid human embryonic cells that identified transcriptional signatures consistent with an alteration of cell proliferation (Martin et al., 2023; Maxwell et al., 2022; Starostik et al., 2020), the cell cycle (Fuchs Weizman et al., 2019; Licciardi et al., 2018; Martin et al., 2023; Starostik et al., 2020; Vera-Rodriguez et al., 2015), deregulation of autophagy (Licciardi et al., 2018; Sanchez-Ribas et al., 2019), p53 signalling (Licciardi et al., 2018) and apoptosis (Groff et al., 2019; Licciardi et al., 2018; Martin et al., 2023; Maxwell et al., 2022; Sanchez-Ribas et al., 2019).

We found that strength of these transcriptomic alterations is dependent of the number of imbalanced genes. These gene-dosage dependent effects of aneuploidy are akin to those extensively reported in human and mouse aneuploid cancer cell lines (Dürrbaum and Storchová, 2016). We found that higher numbers of aneuploid loci led to stronger induction of p53 target genes and apoptosis responses in the TE cells. Interestingly, high-dosage aneuploid embryos displayed an inhibited unfolded protein response, as also seen in aneuploid embryonic cells by another study (Fernandez Gallardo et al., 2023), while this pathway was activated in low dosage aneuploid embryos. These results suggest that while low-dosage aneuploid cells are trying to restore homeostasis by the unfolded protein response (Hetz et al., 2020; Jäger et al., 2012; Li and Zhu, 2022), high-dosage aneuploid cells are past this point and undergo apoptosis by p53 activation.

In the subsequent experiments, we found that aneuploid embryos showed increased signal of early (CASP8) and late (CASP3/7) caspases, indicating activation of the extrinsic apoptotic pathway (McIlwain et al., 2013). The higher levels of p62 and LC3B we found in these embryos suggests that this activation of apoptosis results at least in part from a sustained interaction between p62, LC3B and CASP8 (Pan et al., 2011). In parallel, aneuploid embryos showed evidence of an activated p53 pathway, not only on a transcriptomic level, but also by presenting elevated levels of Serine 15 phosphorylated p53 (Loughery et al., 2014). This p53 activation has been previously observed on a transcriptomic level in another study on human embryos (Licciardi et al., 2018)

and was identified as a key mediator of aneuploidy-dependent apoptosis in the mouse (Singla et al., 2020). While ATM-mediated phosphorylation of p53 on S15 has been reported in cancer cell lines as a consequence of DNA damage during chromosome mis-segregation (Janssen et al., 2011), we found no evidence of increased levels of DNA-damage in our cohort of embryos. It is worth noting that studies on constitutionally aneuploid cell lines have shown contradicting results, with some studies finding p53 activation (Li et al., 2010; Thompson and Compton, 2010) and others not (Tang et al., 2011). An alternative route for p53 activation is through p38, a sensor for cellular stress such as endoplasmic reticulum stress (Mishra and Karande, 2014; Thompson and Compton, 2010). Metabolic alterations might also promote ATM mediated activation of p53 (Li et al., 2010) or phosphorylation on Serine 15 (Jones et al., 2005). Our study also identified *DRAM1* as a significantly upregulated gene in aneuploid embryos. *DRAM1* is directly regulated by p53 and is not only able to regulate autophagic flux but it also regulates apoptosis, making it likely an important downstream effector of the p53-mediated effects of aneuploidy in human embryos (Crighton et al., 2006; Guan et al., 2015). Lastly, it is worth considering that the complex abnormal human embryonic cells present in our sample might have been subjected to mitotic stress, as suggested by the enrichment of mitotic spindle pathway genes observed in the RNA-seq dataset. Mitotic stress might be induced by sustained proteotoxic stress (Zhu et al., 2018) and can further have contributed to p53 activation. Based on this evidence, we propose that the p53 activation we observed in the embryos with presumed meiotic aneuploidy is akin to that of constitutionally aneuploid cells, and not due to DNA-damage but to cellular stress caused by proteotoxic stress. Taken together, the increased levels of apoptosis we find in aneuploid embryos appear to be mediated at least by two pathways: the sustained p62/LC3B mediated response to unfolded proteins and by p53 activation as a response to cellular stress. An interesting observation from the apoptosis stainings is that aneuploid embryos contained increased numbers of CASP3/7 positive micronuclei. This is similar to findings in a non-human primate model showing that abnormal chromosomes can be encapsulated in micronuclei, which can subsequently be selectively eliminated from the embryo (Daughtry et al., 2019). The presence of DNA in the cytoplasm has also recently been observed during live-imaging of human embryos, which occurs during blastocyst expansion due to nuclear DNA shedding (Domingo-Muelas *et al*., 2023). In human cleavage stage embryos these micronuclei have been shown to contain genetic material that originates from chromosome breakages due to replication fork stalling and DNA-damage (Palmerola et al., 2022).

In the second part of our work, we focused on studying the lineage-specific response to complex aneuploidy, as the studies on reversine-treated mouse embryos (Bolton et al., 2016; Singla et al., 2020) and human 2D gastruloids (Yang et al., 2021) also identified a cell-type specific effect of aneuploidy. In the mouse, aneuploid cells are eliminated by apoptosis in the EPI, while tolerated in the TE, and in human 2D gastruloids, aneuploid cells are eliminated in the post-gastrulation embryonic germ layers but tolerated in the TE. In the human embryo, the first lineage segregation is established at 5dpf, and the ICM and TE are marked by the differential expression of NANOG and GATA3 (Gerri et al., 2020; Meistermann et al., 2021; Allègre et al., 2022; Regin et al., 2023). We found that both aneuploid ICM and TE cells showed nuclear enrichment of NANOG, which can be suggestive of a delay or impairment of the first lineage segregation event, possibly due to failure or delay in the exit from pluripotency (Zhang et al., 2016).

While we found increased apoptosis in the aneuploid TE, we found that the ICM/EPI had no CASP3/7 positive cells, despite showing lower cell numbers than the euploid ICM/EPI. These results are in line with the findings of Martin and colleagues, where the RNA-sequencing of TE and ICM samples showed disrupted regulation of apoptosis in mosaic aneuploid TE cells while the ICM showed primarily deregulated mitochondrial function (Martin et al., 2023). In contrast, while the study of Victor et al also finds increased apoptosis in the aneuploid TE, some of their embryos did present CASP3/7 positive signals in the ICM. Further research will be needed to understand if the differences with our findings and those of Martin et al are related to technical or to biological factors. A potential explanation for the lack of apoptosis in the human ICM/EPI could be due to an

uncoupling between aneuploidy-induced stress signals and apoptosis, as observed in human embryonic stem cells (Mantel et al., 2007). In this context, the lower cell numbers in the aneuploid ICM/EPI could be explained by other known effects of *p53* activation next to induction of apoptosis. First, *p53* activation can decrease cell proliferation, leading to lower cell numbers. Secondly, *p53* activation can downregulate *NANOG* expression (Abdelalim and Tooyama, 2014; Lin et al., 2005), potentially leading to loss of pluripotency and driving the cells to differentiation and out of the ICM/EPI.

Another observation was that while the aneuploid TE had increased levels of autophagy markers and DRAM1 expression, this did not reach statistical significance in the ICM/EPI. This aligns with work on human embryos showing absence of activation of p53-signalling and autophagy in the transcriptome of the ICM of mosaic human embryos (Martin et al., 2023), but is in contrast with the reversine-treated mouse embryos and human gastruloids, showing increased autophagy and p53 signalling in the ICM lineages (Singla et al., 2020; Yang et al., 2021). Next to a species-specific effect, it is possible that the difference between the mouse, human gastruloid and human studies are because the reversine treatment used had direct effects on p53 (D'Alise et al., 2008; S Santaguida, 2010), leading to the activation of autophagy across the entire cells.

Finally, we found that in those embryos that had already undergone the second lineage segregation event, the aneuploid embryos had a significantly lower ratio of PrE (GATA4-positive) to EPI (OCT4-positive/GATA4-negative) cells than euploid embryos, suggesting that aneuploidy has a negative effect on PrE formation. Interestingly, recent work comparing the gene-expression of euploid and mosaic aneuploid embryos has also found that euploid embryos have a higher expression of the PrE marker *SOX17*, (Martin et al., 2023).

While in mice, apoptosis is common during PrE formation to eliminate misallocated cells through cell competition (Hashimoto and Sasaki, 2019; Plusa et al., 2008), our data and that of others suggest that the human ICM rarely undergoes apoptosis, even in karyotypically aberrant cells (Martin et al., 2023; Victor et al., 2019; Yang et al., 2021). While a possible explanation suggested by our NANOG stainings is that in aneuploid human embryos the PrE forms later due to retention of NANOG in the ICM and TE, the mechanisms behind this second lineage differentiation defect remain to be elucidated.

When interpreting the results of this study, it is important to bear in mind that we identified the ICM/EPI as staining positive for OCT4 and the PrE as positive for GATA4. We confirmed that the embryos analysed were expanded blastocysts which had undergone the first lineage segregations, as OCT4 was restricted to the inner cells and absent in TE cells (Niakan and Eggan, 2013). The identity of human ICM and EPI cells is currently under vigorous debate (Meistermann et al., 2021; Radley et al., 2022) and exclusive markers of either cell type are untested. Therefore, we cannot assign ICM or EPI identity to OCT4-positive cells with certainty. However, in blastocysts with GATA4-positive cells the second lineage segregation had occurred and PrE was established, and consequently we confidently assigned the EPI identity to OCT4-positive cells in these blastocysts. In GATA4-negative embryos OCT4-positive cells could be either ICM or EPI cells. Interestingly, we only found a single GATA4-positive cell lacking OCT4, supporting the hypothesis that PrE cells differentiate from EPI cells (Meistermann et al., 2021).

Our study has several limitations and there are some considerations to bear in mind. In this work, we did not analyse the transcriptome of the ICM, because the remaining embryos were used for immunostaining after TE biopsy, and we can therefore not draw any conclusions on the ICM transcriptome. We did not study embryos with the same type of aneuploidy and can thus not provide insight on chromosome-specific effects. Although some of our embryos carried genetic abnormalities in mosaic form as part of their complex karyotype (aneuploid/aneuploid mosaics), we did not study diploid/aneuploid mosaic embryos and can therefore not assert that these also activate the same cellular stress pathways in their aneuploid cells. Since these pathways are

common to most cell types, our prediction would however be that they are activated in mosaic embryos too. The possibilities for functional studies and lineage tracing experiments in human embryos are very limited, which is why we can only present an observational study. Alternatively, in silico modelling data could be leveraged to address the roles of aneuploidy in blastocyst formation and development (Nissen et al., 2017). The gene-expression analysis revealed that embryos with naturally acquired and induced aneuploidies had few deregulated pathways in common, with mainly the mitotic spindle genes being differentially expressed in both. Conversely, we used reversine to induce aneuploidy in the immunostaining experiments to increase the sample size, and the results showed that the reversine-induced aneuploidies elicited the same stress responses as aneuploidy. This suggests that while reversine-based models are very close, they may not fully mimic endogenous aneuploidy. An alternative is to use the SAC-inhibitor A3146, recently proposed by the Zernicka-Goetz group to induce low-degree aneuploidy in mouse embryos (Sanchez-Vasquez et al., 2023). Finally, our results on the activation of autophagy and proteotoxic stress are also limited by experimental constraints. We cannot rule out indirect activation of apoptosis mediated by autophagy due to the degradation of cell organelles (Gump and Thorburn, 2011). Also, other upstream regulators of autophagy could be involved, such as the cGAS-STING pathway (Krivega et al., 2021). While we and others (Singla et al., 2020) used HSP70 as a marker for chronic protein misfolding, we cannot preclude that is also acts as a (temporary) suppressor of the extrinsic apoptosis pathway in aneuploid cells (Gabai et al., 2002; Lanneau et al., 2008).

Taken together, our results show that while the same pathways appear to be activated in human and mouse embryos with complex aneuploidy, human embryos have a dosage-dependent and differential response when it comes to the downstream effect of these pathways in the different cell lineages. While the mouse readily depletes aneuploid cells by apoptosis specifically from the embryonic lineage before implantation (Bolton et al., 2016; Singla et al., 2020), in the human embryo, apoptosis appears to be more active in the TE and aneuploidy negatively affects PrE formation in the ICM. Our results provide insight into the mechanisms by which human embryos respond to gene-dosage imbalances and may contribute to understanding how aneuploid cells are selectively eliminated in mosaic preimplantation embryos. Further research, especially by using human embryos with endogenous chromosomal mosaicism, will be needed to shed light on the interactions between proteotoxic stress, the p53 pathway and differentiation during early development, for which the most novel models of human embryo implantation (Deglincerti et al., 2016; Kagawa et al., 2021; Shahbazi et al., 2020, 2016) will prove to be of incalculable value.

Data availability

Data are available from the corresponding author upon reasonable request. Files are stored at the Open Science Framework (OSF) and can be accessed through the identifier: osf.io/tc248. At OSF we provided for **Figure 1**, **2** and **Supplementary Figure 1** the input and output of the GSEA for each comparison. Also, source data files are provided for figures 3 and 4 and Supplementary Figure 2. We also provide the Prism file for all comparisons in which significancy was tested. Raw RNA-sequencing files are not provided due to GDPR guidelines concerning human embryo research. However, count tables generated from the raw data files are included in the source data files.

Acknowledgements

The authors would like to thank Marleen Carlé from the Center for Medical Genetics (UZ Brussel) for assisting during the tubing of trophectoderm samples, Hanne Vlieghe (UCLouvain, Brussels) for the validation of antibodies and the reversine reagent, Wilfried Cools from the Biostatistics and Medical Informatics Group (VUB) for the statistical advice and the members of the BRIGHTcore facility (UZ Brussel) for performing the RNA sequencing. We thank Prof. Rajiv McCoy for the scientific input and data exchange. This study was funded by the Fonds for Scientific Research in Flanders -G017218N-(Fonds Wetenschappelijk Onderzoek – Vlaanderen [FWO]). M.R., E.C.D.D. and C.J. are doctoral fellows at the FWO with grant numbers (1133622N, 1S73521N and 11H9823N, respectively). Y.L. is a predoctoral fellow supported by the China Scholarship Council (CSC)

Additional information

Author contributions

M.R. carried out all the experiments unless stated otherwise, interpreted, and analyzed the results, revised, and co-wrote the manuscript. Y.L. and E.C.D.D. performed bioinformatics analyses. C.J. contributed to immunostaining experiments during the revision. A.H. contributed to quantifications during the revision. Y.G. performed the trophectoderm biopsies. P.V. provided and supervised the diagnoses of the PGT embryos. G.V. and H.V.D.V. provided the embryos for this study. K.S. interpreted and supervised the experimental work and co-wrote the manuscript. C.S. designed, interpreted and supervised the experimental work and co-wrote the manuscript. All co-authors proofread the manuscript.

Competing interests

The authors declare no competing interests.

Supplementary Fig. 1

Expanded RNA-sequencing analysis

a. Principal component analysis of reversine versus euploid embryos. **b.** InferCNV analysis of individual euploid samples compared to the reference set. **c.** InferCNV analysis of individual reversine samples compared to the reference set. **d**. Volcano plot after differential gene expression analysis with a cutoff value of $|\log_2$ fold change$| > 1$ and $-\log_{10}(FDR) < 0.05$ for reversine versus euploid embryos showing 34 upregulated and 22 downregulated genes. **e.** Barplot of enriched Hallmark pathways after gene set enrichment analysis of reversine versus euploid embryos using a cut-off value of 25% FDR. **f.** Barplot of TOP20 enriched C2 library pathways after gene set enrichment analysis of reversine versus euploid embryos using a cut-off value of 25% FDR. Source of all embryos: Experiment 1.

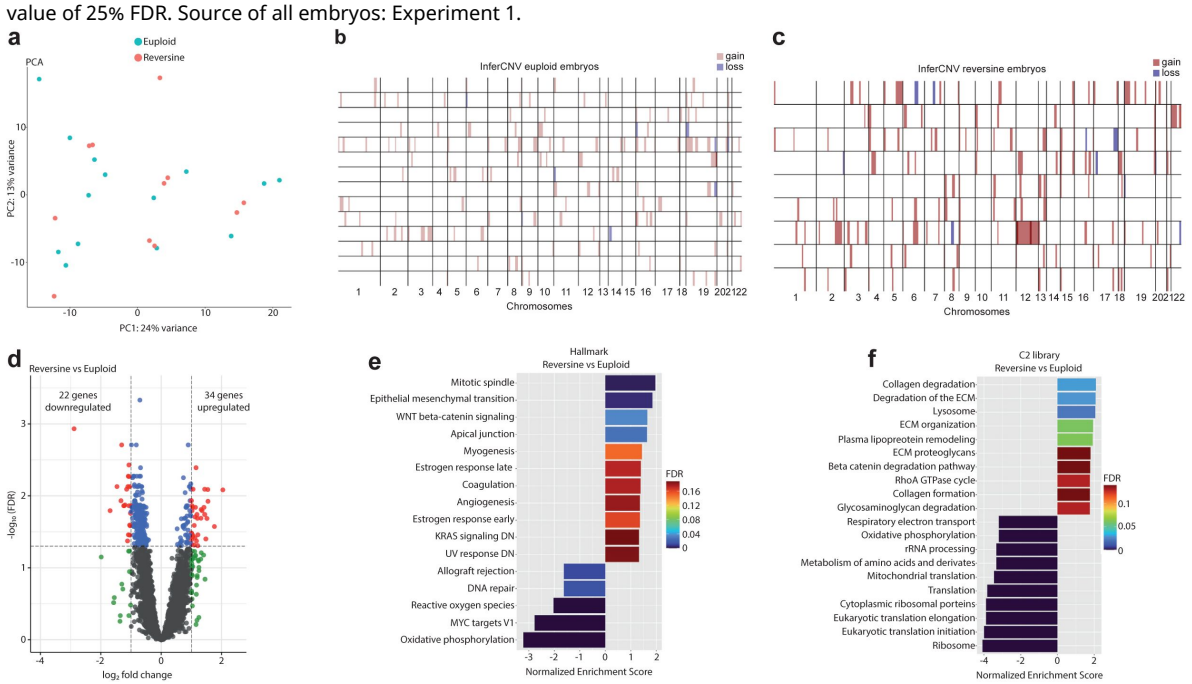

Supplementary Fig. 2

S15-p53 expression in TE vs OCT4-positive cells (ICM/EPI) in aneuploid embryos

a, Orthogonal projections after immunostaining of euploid and aneuploid embryos for DNA (white), S15p53 (turquoise) and OCT4 (magenta). **b**, Percentages of nuclei positive for S15p53 per embryo in euploid (n = 3) and aneuploid (n = 4) embryos in the ICM. **c**, Percentages of nuclei positive for S15p53 per embryo in euploid (n = 3) and aneuploid (n = 5) embryos in the TE. Brightfield pictures were obtained during confocal imaging. All scale bars are 20 µm. Box and plots show median and minimum to maximum values. Bar plots show mean ± s.d. For all plots each dot represents a single embryo. Source of all embryos: Experiment 4.

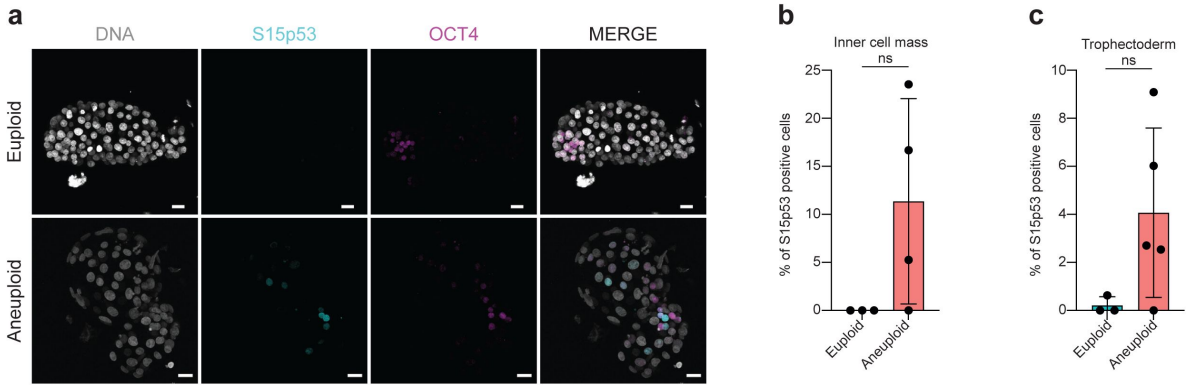

References

Abdelalim EM, Tooyama I (2014) **Knockdown of p53 suppresses Nanog expression in embryonic stem cells** *Biochem Biophys Res Commun* **443**:652–657 https://doi.org/10.1016/J.BBRC.2013.12.030

Allègre N, Chauveau S, Dennis C, Renaud Y, Meistermann D, Estrella LV, Pouchin P, Cohen-Tannoudji M, David L, Chazaud C (2022) **NANOG initiates epiblast fate through the coordination of pluripotency genes expression** *Nature Communications* **13**:1–13 https://doi.org/10.1038/s41467-022-30858-8

Ariyoshi K, Miura T, Kasai K, Fujishima Y, Oshimura M, Yoshida MA (2016) **Induction of genomic instability and activation of autophagy in artificial human aneuploid cells** *Mutat Res* **790**:19–30 https://doi.org/10.1016/J.MRFMMM.2016.06.001

Bolton H, Graham SJL, Van Der Aa N, Kumar P, Theunis K, Fernandez Gallardo E, Voet T, Zernicka-Goetz M. (2016) **Mouse model of chromosome mosaicism reveals lineage-specific depletion of aneuploid cells and normal developmental potential** *Nat Commun* **7**:1–12 https://doi.org/10.1038/ncomms11165

Capalbo A *et al.* (2021) **Mosaic human preimplantation embryos and their developmental potential in a prospective, non-selection clinical trial** *The American Journal of Human Genetics* **108**:2238–2247 https://doi.org/10.1016/j.ajhg.2021.11.002

Capalbo A, Wright G, Elliott T, Ubaldi FM, Rienzi L, Nagy ZP (2013) **FISH reanalysis of inner cell mass and trophectoderm samples of previously array-CGH screened blastocysts shows high accuracy of diagnosis and no major diagnostic impact of mosaicism at the blastocyst stage** *Human Reproduction* **28**:2298–2307 https://doi.org/10.1093/humrep/det245

Chavez SL, Loewke KE, Han J, Moussavi F, Colls P, Munne S, Behr B, Reijo Pera RA (2012) **Dynamic blastomere behaviour reflects human embryo ploidy by the four-cell stage** *Nat Commun* **3** https://doi.org/10.1038/NCOMMS2249

Chow JFC, Yeung WSB, Lau EYL, Lee VCY, Ng EHY, Ho PC (2014) **Array comparative genomic hybridization analyses of all blastomeres of a cohort of embryos from young IVF patients revealed significant contribution of mitotic errors to embryo mosaicism at the cleavage stage** *Reprod Biol Endocrinol* **12** https://doi.org/10.1186/1477-7827-12-105

Chunduri NK, Barthel K, Storchova Z (2022) **Consequences of Chromosome Loss: Why Do Cells Need Each Chromosome Twice?** *Cells 2022* **11** https://doi.org/10.3390/CELLS11091530

Chunduri NK, Storchová Z (2019) **The diverse consequences of aneuploidy** *Nat Cell Biol* https://doi.org/10.1038/s41556-018-0243-8

Coorens THH *et al.* (2021) **Inherent mosaicism and extensive mutation of human placentas** *Nature* **592**:80–85 https://doi.org/10.1038/s41586-021-03345-1

Crighton D, Wilkinson S, O'Prey J, Syed N, Smith P, Harrison PR, Gasco M, Garrone O, Crook T, Ryan KM (2006) **DRAM, a p53-Induced Modulator of Autophagy, Is Critical for Apoptosis** *Cell* **126**:121–134 https://doi.org/10.1016/j.cell.2006.05.034

Currie CE, Ford E, Benham Whyte L, Taylor DM, Mihalas BP, Erent M, Marston AL, Hartshorne GM, McAinsh AD (2022) **The first mitotic division of human embryos is highly error prone** *Nat Commun* **13** https://doi.org/10.1038/S41467-022-34294-6

D'Alise AM, Amabile G, Iovino M, Di Giorgio FP, Bartiromo M, Sessa F, Villa F, Musacchio A, Cortese R. (2008) **Reversine, a novel Aurora kinases inhibitor, inhibits colony formation of human acute myeloid leukemia cells** *Mol Cancer Ther* **7**:1140–1149 https://doi.org/10.1158/1535-7163.MCT-07-2051

Dang C V., O'Donnell KA, Zeller KI, Nguyen T, Osthus RC, Li F (2006) **The c-Myc target gene network** *Semin Cancer Biol* **16**:253–264 https://doi.org/10.1016/J.SEMCANCER.2006.07.014

Daughtry BL *et al.* (2019) **Single-cell sequencing of primate preimplantation embryos reveals chromosome elimination via cellular fragmentation and blastomere exclusion** *Genome Res* **29**:367–382 https://doi.org/10.1101/gr.239830.118

Gardner David K, Schoolcraft William B (1999) **Culture and transfer of human blastocysts** *Curr Opin Obstet Gynecol* **11**:307–311

Deglincerti A, Croft GF, Pietila LN, Zernicka-Goetz M, Siggia ED, Brivanlou AH (2016) **Self-organization of the in vitro attached human embryo** *Nature* **533**:251–254 https://doi.org/10.1038/nature17948

Dobin A, Davis CA, Schlesinger F, Drenkow J, Zaleski C, Jha S, Batut P, Chaisson M, Gingeras TR (2013) **STAR: ultrafast universal RNA-seq aligner** *Bioinformatics* **29**:15–21 https://doi.org/10.1093/bioinformatics/bts635

Donnelly N, Passerini V, Dürrbaum M, Stingele S, Storchová Z (2014) **HSF1 deficiency and impaired HSP90-dependent protein folding are hallmarks of aneuploid human cells** *EMBO J* **33** https://doi.org/10.15252/EMBJ.201488648

Dürrbaum M, Kuznetsova A, Passerini V, Stingele S, Stoehr G, Storchová Z (2014) **Unique features of the transcriptional response to model aneuploidy in human cells** *BMC Genomics* **15** https://doi.org/10.1186/1471-2164-15-139

Dürrbaum M, Storchová Z (2016) **Effects of aneuploidy on gene expression: implications for cancer** *FEBS J* **283**:791–802 https://doi.org/10.1111/FEBS.13591

Fernandez Gallardo E *et al.* (2023) **A multi-omics genome-and-transcriptome single-cell atlas of human preimplantation embryogenesis reveals the cellular and molecular impact of chromosome instability** *bioRxiv* https://doi.org/10.1101/2023.03.08.530586

Fragouli E, Alfarawati S, Spath K, Babariya D, Tarozzi N, Borini A, Wells D (2017) **Analysis of implantation and ongoing pregnancy rates following the transfer of mosaic diploid–aneuploid blastocysts** *Hum Genet* **136**:805–819 https://doi.org/10.1007/s00439-017-1797-4

Fragouli E, Munne S, Wells D (2019) **The cytogenetic constitution of human blastocysts: insights from comprehensive chromosome screening strategies** *Hum Reprod Update* **25**:15–33 https://doi.org/10.1093/humupd/dmy036

Weizman N Fuchs, Wyse BA, Antes R, Ibarrientos Z, Sangaralingam M, Motamedi G, Kuznyetsov V, Madjunkova S, Librach CL (2019) **Towards Improving Embryo Prioritization: Parallel Next Generation Sequencing of DNA and RNA from a Single Trophectoderm Biopsy** *Sci Rep* **9**:1–11 https://doi.org/10.1038/s41598-019-39111-7

Gabai VL, Mabuchi K, Mosser DD, Sherman MY (2002) **Hsp72 and Stress Kinase c-jun N-Terminal Kinase Regulate the Bid-Dependent Pathway in Tumor Necrosis Factor-Induced Apoptosis** *Mol Cell Biol* **22** https://doi.org/10.1128/MCB.22.10.3415-3424.2002

Gerri C *et al.* (2020) **Initiation of a conserved trophectoderm program in human, cow and mouse embryos** *Nature* **587**:443–447 https://doi.org/10.1038/S41586-020-2759-X

Greco E, Minasi MG, Fiorentino F (2015) **Healthy Babies after Intrauterine Transfer of Mosaic Aneuploid Blastocysts** *New England Journal of Medicine* **373**:2089–2090 https://doi.org/10.1056/NEJMc1500421

Griffin DK, Brezina PR, Tobler K, Zhao Y, Silvestri G, Mccoy RC, Anchan R, Benner A, Cutting GR, Kearns WG (2022) **The human embryonic genome is karyotypically complex, with chromosomally abnormal cells preferentially located away from the developing fetus** *Human Reproduction* https://doi.org/10.1093/HUMREP/DEAC238

Groff AF, Resetkova N, DiDomenico F, Sakkas D, Penzias A, Rinn JL, Eggan K (2019) **RNA-seq as a tool for evaluating human embryo competence** *Genome Res* **29**:1705–1718 https://doi.org/10.1101/gr.252981.119

Guan JJ, Zhang XD, Sun W, Qi L, Wu JC, Qin ZH (2015) **DRAM1 regulates apoptosis through increasing protein levels and lysosomal localization of BAX** *Cell Death Dis* **6**:e1624–e1624 https://doi.org/10.1038/cddis.2014.546

Gump JM, Thorburn A (2011) **Autophagy and apoptosis: what is the connection?** *Trends Cell Biol* **21**:387–392 https://doi.org/10.1016/J.TCB.2011.03.007

Hashimoto M, Sasaki H (2019) **Epiblast Formation by TEAD-YAP-Dependent Expression of Pluripotency Factors and Competitive Elimination of Unspecified Cells** *Dev Cell* **50**:139–154 https://doi.org/10.1016/J.DEVCEL.2019.05.024

Hetz C, Zhang K, Kaufman RJ (2020) **Mechanisms, regulation and functions of the unfolded protein response** *Nature Reviews Molecular Cell Biology* **21**:421–438 https://doi.org/10.1038/s41580-020-0250-z

Huettel B, Kreil DP, Matzke M, Matzke AJM (2008) **Effects of aneuploidy on genome structure, expression, and interphase organization in Arabidopsis thaliana** *PLoS Genet* **4** https://doi.org/10.1371/JOURNAL.PGEN.1000226

Hung CM, Garcia-Haro L, Sparks CA, Guertin DA (2012) **mTOR-Dependent Cell Survival Mechanisms** *Cold Spring Harb Perspect Biol* **4** https://doi.org/10.1101/CSHPERSPECT.A008771

Jacobs K, Van de Velde H, De Paepe C, Sermon K, Spits C. (2017) **Mitotic spindle disruption in human preimplantation embryos activates the spindle assembly checkpoint but not apoptosis until Day 5 of development** *MHR: Basic science of reproductive medicine* **23**:321–329 https://doi.org/10.1093/molehr/gax007

Jäger R, Bertrand MJM, Gorman AM, Vandenabeele P, Samali A (2012) **The unfolded protein response at the crossroads of cellular life and death during endoplasmic reticulum stress** *Biol Cell* **104**:259–270 https://doi.org/10.1111/BOC.201100055

Janssen A, Van Der Burg M, Szuhai K, Kops GJPL, Medema RH. (2011) **Chromosome segregation errors as a cause of DNA damage and structural chromosome aberrations** *Science* **333**:1895–1898 https://doi.org/10.1126/SCIENCE.1210214

Johnson DS, Cinnioglu C, Ross R, Filby A, Gemelos G, Hill M, Ryan A, Smotrich D, Rabinowitz M, Murray MJ (2010) **Comprehensive analysis of karyotypic mosaicism between trophectoderm and inner cell mass** *MHR: Basic science of reproductive medicine* **16**:944–949 https://doi.org/10.1093/molehr/gaq062

Jones RG, Plas DR, Kubek S, Buzzai M, Mu J, Xu Y, Birnbaum MJ, Thompson CB (2005) **AMP-activated protein kinase induces a p53-dependent metabolic checkpoint** *Mol Cell* **18**:283–293 https://doi.org/10.1016/J.MOLCEL.2005.03.027

Kagawa H *et al.* (2021) **Human blastoids model blastocyst development and implantation** *Nature* :1–9 https://doi.org/10.1038/s41586-021-04267-8

Kalousek DK, Vekemans M (1996) **Confined placental mosaicism** *J Med Genet* https://doi.org/10.1136/jmg.33.7.529

Krivega M, Stiefel CM, Karbassi S, Andersen LL, Chunduri NK, Donnelly N, Pichlmair A, Storchová Z (2021) **Genotoxic stress in constitutive trisomies induces autophagy and the innate immune response via the cGAS-STING pathway** *Communications Biology* **4**:1–16 https://doi.org/10.1038/s42003-021-02278-9

Krivega M, Stiefel CM, Storchova Z (2022) **Consequences of chromosome gain: A new view on trisomy syndromes** *Am J Hum Genet* https://doi.org/10.1016/j.ajhg.2022.10.014

Lanneau D, Brunet M, Frisan E, Solary E, Fontenay M, Garrido C (2008) **Heat shock proteins: essential proteins for apoptosis regulation** *J Cell Mol Med* **12** https://doi.org/10.1111/J.1582-4934.2008.00273.X

Li B, Dewey CN (2011) **RSEM: accurate transcript quantification from RNA-Seq data with or without a reference genome** *BMC Bioinformatics* **12**

Li M, Fang X, Baker DJ, Guo L, Gao X, Wei Z, Han S, Van Deursen JM, Zhang P. (2010) **The ATM-p53 pathway suppresses aneuploidy-induced tumorigenesis** *Proc Natl Acad Sci U S A* **107**:14188–14193 https://doi.org/10.1073/PNAS.1005960107/SUPPL_FILE/PNAS.201005960SI.PDF

Li R, Zhu J (2022) **Effects of aneuploidy on cell behaviour and function** *Nature Reviews Molecular Cell Biology* **23**:250–265 https://doi.org/10.1038/s41580-021-00436-9

Licciardi F, Lhakhang T, Kramer YG, Zhang Y, Heguy A, Tsirigos A. (2018) **Human blastocysts of normal and abnormal karyotypes display distinct transcriptome profiles** *Sci Rep* **8**:1–9 https://doi.org/10.1038/s41598-018-33279-0

Lin T, Chao C, Saito S, Mazur SJ, Murphy ME, Appella E, Xu Y (2005) **p53 induces differentiation of mouse embryonic stem cells by suppressing Nanog expression** *Nat Cell Biol* **7**:165–171 https://doi.org/10.1038/NCB1211

Loughery J, Cox M, Smith LM, Meek DW (2014) **Critical role for p53-serine 15 phosphorylation in stimulating transactivation at p53-responsive promoters** *Nucleic Acids Res* **42**:7666–7680 https://doi.org/10.1093/nar/gku501

Love MI, Huber W, Anders S (2014) **Moderated estimation of fold change and dispersion for RNA-seq data with DESeq2** *Genome Biol* **15** https://doi.org/10.1186/s13059-014-0550-8

Mantel C *et al.* (2007) **Checkpoint-apoptosis uncoupling in human and mouse embryonic stem cells: a source of karyotpic instability** *Blood* **109**:4518–4527 https://doi.org/10.1182/blood-2006-10

Martin A, Mercader A, Dominguez F, Quiñonero A, Perez M, Gonzalez-Martin R, Delgado A, Mifsud A, Pellicer A, De Los Santos MJ. (2023) **Mosaic results after preimplantation genetic testing for aneuploidy may be accompanied by changes in global gene expression** *Front Mol Biosci* **10** https://doi.org/10.3389/FMOLB.2023.1180689

Maxwell SM, Lhakhang TC, Lin Z, Kramer YG, Zhang Y, Wang F, Heguy A, Tsirigos A, Grifo JA, Licciardi F (2022) **Investigation of Global Gene Expression of Human Blastocysts Diagnosed as Mosaic using Next-generation Sequencing** *Reproductive Sciences* :1–11 https://doi.org/10.1007/s43032-022-00899-x

McCoy RC (2017) **Mosaicism in Preimplantation Human Embryos: When Chromosomal Abnormalities Are the Norm** *Trends in Genetics* **33**:448–463 https://doi.org/10.1016/J.TIG.2017.04.001

McIlwain DR, Berger T, Mak TW (2013) **Caspase Functions in Cell Death and Disease** *Cold Spring Harb Perspect Biol* **5**:1–28 https://doi.org/10.1101/CSHPERSPECT.A008656

Meistermann D *et al.* (2021) **Integrated pseudotime analysis of human pre-implantation embryo single-cell transcriptomes reveals the dynamics of lineage specification** *Cell Stem Cell* **28**:1625–1640 https://doi.org/10.1016/j.stem.2021.04.027

Mertzanidou A, Spits C, Nguyen HT, Van de Velde H, Sermon K. (2013) **Evolution of aneuploidy up to Day 4 of human preimplantation development** *Human Reproduction* **28**:1716–1724 https://doi.org/10.1093/humrep/det079

Mertzanidou A, Wilton L, Cheng J, Spits C, Vanneste E, Moreau Y, Vermeesch JR, Sermon K (2013) **Microarray analysis reveals abnormal chromosomal complements in over 70% of 14 normally developing human embryos** *Human Reproduction* **28**:256–264 https://doi.org/10.1093/humrep/des362

Mishra R, Karande AA (2014) **Endoplasmic Reticulum Stress-Mediated Activation of p38 MAPK, Caspase-2 and Caspase-8 Leads to Abrin-Induced Apoptosis** *PLoS One* **9** https://doi.org/10.1371/JOURNAL.PONE.0092586

Munné S *et al.* (2017) **Detailed investigation into the cytogenetic constitution and pregnancy outcome of replacing mosaic blastocysts detected with the use of high-resolution next-generation sequencing** *Fertil Steril* **108**:62–71 https://doi.org/10.1016/j.fertnstert.2017.05.002

Munné S *et al.* (2020) **First PGT-A using human in vivo blastocysts recovered by uterine lavage: Comparison with matched IVF embryo controls** *Human Reproduction* **35**:70–80 https://doi.org/10.1093/humrep/dez242

Munné S, Spinella F, Grifo J, Zhang J, Beltran MP, Fragouli E, Fiorentino F (2020) **Clinical outcomes after the transfer of blastocysts characterized as mosaic by high resolution Next Generation Sequencing-further insights** *Eur J Med Genet* **63** https://doi.org/10.1016/j.ejmg.2019.103741

Niakan KK, Eggan K (2013) **Analysis of human embryos from zygote to blastocyst reveals distinct gene expression patterns relative to the mouse** *Dev Biol* **375**:54–64 https://doi.org/10.1016/J.YDBIO.2012.12.008

Nissen SB, Perera M, Gonzalez JM, Morgani SM, Jensen MH, Sneppen K, Brickman JM, Trusina A (2017) **Four simple rules that are sufficient to generate the mammalian blastocyst** *PLoS Biol* **15** https://doi.org/10.1371/JOURNAL.PBIO.2000737

Ohashi A *et al.* (2015) **Aneuploidy generates proteotoxic stress and DNA damage concurrently with p53-mediated post-mitotic apoptosis in SAC-impaired cells** *Nat Commun* **6**:1–16 https://doi.org/10.1038/ncomms8668

Oromendia AB, Dodgson SE, Amon A (2012) **Aneuploidy causes proteotoxic stress in yeast** *Genes Dev* **26**:2696–2708 https://doi.org/10.1101/gad.207407.112

Orvieto R, Shimon C, Rienstein S, Jonish-Grossman A, Shani H, Aizer A (2020) **Do human embryos have the ability of self-correction?** *Reprod Biol Endocrinol* **18** https://doi.org/10.1186/S12958-020-00650-8

Palmerola KL *et al.* (2022) **Replication stress impairs chromosome segregation and preimplantation development in human embryos** *Cell* https://doi.org/10.1016/j.cell.2022.06.028

Pan J-A, Ullman E, Dou Z, Zong W-X (2011) **Inhibition of protein degradation induces apoptosis through a microtubule-associated protein 1 light chain 3-mediated activation of caspase-8 at intracellular membranes** *Mol Cell Biol* **31**:3158–70 https://doi.org/10.1128/MCB.05460-11

Passerini V, Ozeri-Galai E, De Pagter MS, Donnelly N, Schmalbrock S, Kloosterman WP, Kerem B, Storchová Z. (2016) **The presence of extra chromosomes leads to genomic instability** *Nat Commun* **7** https://doi.org/10.1038/NCOMMS10754

Plusa B, Piliszek A, Frankenberg S, Artus J, Hadjantonakis AK (2008) **Distinct sequential cell behaviours direct primitive endoderm formation in the mouse blastocyst** *Development* **135**:3081–3091 https://doi.org/10.1242/DEV.021519

Popovic M, Dhaenens L, Boel A, Menten B, Heindryckx B (2020) **Chromosomal mosaicism in human blastocysts: The ultimate diagnostic dilemma** *Hum Reprod Update* **26**:313–334 https://doi.org/10.1093/humupd/dmz050

Popovic M *et al.* (2018) **Chromosomal mosaicism in human blastocysts: The ultimate challenge of preimplantation genetic testing?** *Human Reproduction* **33**:1342–1354 https://doi.org/10.1093/humrep/dey106

Radley A, Corujo-Simon E, Nichols J, Smith A, Dunn SJ (2022) **Entropy sorting of single-cell RNA sequencing data reveals the inner cell mass in the human pre-implantation embryo** *Stem Cell Reports* 0 https://doi.org/10.1016/j.stemcr.2022.09.007

Regin M *et al.* (2023) **Lineage segregation in human pre-implantation embryos is specified by YAP1 and TEAD1** *Human Reproduction* **38**:1484–1498 https://doi.org/10.1093/HUMREP/DEAD107

Regin M, Spits C, Sermon K (2022) **On the origins and fate of chromosomal abnormalities in human preimplantation embryos: an unsolved riddle** *Mol Hum Reprod* https://doi.org/10.1093/molehr/gaac011

Ren Y *et al.* (2022) **Regional and developmental characteristics of human embryo mosaicism revealed by single cell sequencing** *PLoS Genet* **18** https://doi.org/10.1371/journal.pgen.1010310

Ritchie ME, Phipson B, Wu D, Hu Y, Law CW, Shi W, Smyth GK (2015) **Limma powers differential expression analyses for RNA-sequencing and microarray studies** *Nucleic Acids Res* **43** https://doi.org/10.1093/nar/gkv007

Robinson MD, McCarthy DJ, Smyth GK (2009) **edgeR: A Bioconductor package for differential expression analysis of digital gene expression data** *Bioinformatics* **26**:139–140 https://doi.org/10.1093/BIOINFORMATICS/BTP616

Robinson MD, Oshlack A (2010) **A scaling normalization method for differential expression analysis of RNA-seq data** *Genome Biol* **11** https://doi.org/10.1186/gb-2010-11-3-r25

S Santaguida ATADSTAM (2010) **Dissecting the role of MPS1 in chromosome biorientation and the spindle checkpoint through the small molecule inhibitor reversine** *J Cell Biol* **190**:73–87

Sanchez-Ribas I, Diaz-Gimeno P, Sebastián-León P, Mercader A, Quiñonero A, Ballesteros A, Pellicer A, Domínguez F (2019) **Transcriptomic behavior of genes associated with chromosome 21 aneuploidies in early embryo development** *Fertil Steril* **111**:991–1001 https://doi.org/10.1016/j.fertnstert.2019.01.023

Sanchez-Vasquez E, Bronner ME, Zernicka-Goetz M. (2023) **HIF1A contributes to the survival of aneuploid and mosaic pre-implantation embryos** *bioRxiv* https://doi.org/10.1101/2023.09.04.556218

Santaguida S, Amon A (2015) **Short- and long-term effects of chromosome mis-segregation and aneuploidy** *Nat Rev Mol Cell Biol* https://doi.org/10.1038/nrm4025

Santaguida S, Richardson A, Iyer DR, M'Saad O, Zasadil L, Knouse KA, Wong YL, Rhind N, Desai A, Amon A (2017) **Chromosome Mis-segregation Generates Cell-Cycle-Arrested Cells with Complex Karyotypes that Are Eliminated by the Immune System** *Dev Cell* **41**:638–651 https://doi.org/10.1016/J.DEVCEL.2017.05.022

Santaguida S, Vasile E, White E, Amon A (2015) **Aneuploidy-induced cellular stresses limit autophagic degradation** *Genes Dev* **29**:2010–2021 https://doi.org/10.1101/gad.269118.115

Shahbazi MN *et al.* (2016) **Self-organization of the human embryo in the absence of maternal tissues** *Nat Cell Biol* **18**:700–708 https://doi.org/10.1038/ncb3347

Shahbazi MN *et al.* (2020) **Developmental potential of aneuploid human embryos cultured beyond implantation** *Nat Commun* **11**:1–15 https://doi.org/10.1038/s41467-020-17764-7

Sheltzer JM, Blank HM, Pfau SJ, Tange Y, George BM, Humpton TJ, Brito IL, Hiraoka Y, Niwa O, Amon A (2011) **Aneuploidy drives genomic instability in yeast** *Science (1979)* **333**:1026–1030 https://doi.org/10.1126/SCIENCE.1206412/SUPPL_FILE/1206412-SHELTZER.SOM.PDF

Simões-Sousa S *et al.* (2018) **The p38α Stress Kinase Suppresses Aneuploidy Tolerance by Inhibiting Hif-1α** *Cell Rep* **25**:749–760 https://doi.org/10.1016/J.CELREP.2018.09.060

Singla S, Iwamoto-Stohl LK, Zhu M, Zernicka-Goetz M (2020) **Autophagy-mediated apoptosis eliminates aneuploid cells in a mouse model of chromosome mosaicism** *Nat Commun* **11**:1–15 https://doi.org/10.1038/s41467-020-16796-3

Starostik MR, Sosin OA, McCoy RC (2020) **Single-cell analysis of human embryos reveals diverse patterns of aneuploidy and mosaicism** *Genome Res* **30**:814–826 https://doi.org/10.1101/gr.262774.120

Stingele S, Stoehr G, Peplowska K, Cox J, Mann M, Storchova Z (2012) **Global analysis of genome, transcriptome and proteome reveals the response to aneuploidy in human cells** *Mol Syst Biol* **8** https://doi.org/10.1038/msb.2012.40

Tang YC, Williams BR, Siegel JJ, Amon A (2011) **Identification of Aneuploidy-Selective Antiproliferation Compounds** *Cell* **144**:499–512 https://doi.org/10.1016/J.CELL.2011.01.017

Thompson SL, Compton DA (2010) **Proliferation of aneuploid human cells is limited by a p53-dependent mechanism** *J Cell Biol* **188**:369–381 https://doi.org/10.1083/JCB.200905057

Torres EM, Sokolsky T, Tucker CM, Chan LY, Boselli M, Dunham MJ, Amon A (2007) **Effects of aneuploidy on cellular physiology and cell division in haploid yeast** *Science (1979)* **317**:916–924 https://doi.org/10.1126/SCIENCE.1142210/SUPPL_FILE/TORRES.SOM.PDF

van Echten-Arends J, Mastenbroek S, Sikkema-Raddatz B, Korevaar JC, Heineman MJ, van der Veen F, Repping S. (2011) **Chromosomal mosaicism in human preimplantation embryos: a systematic review** *Hum Reprod Update* **17**:620–627 https://doi.org/10.1093/humupd/dmr014

Van Landuyt L, Stoop D, Verheyen G, Verpoest W, Camus M, Van De Velde H, Devroey P, Van Den Abbeel E. (2011) **Outcome of closed blastocyst vitrification in relation to blastocyst quality: Evaluation of 759 warming cycles in a single-embryo transfer policy** *Human Reproduction* **26**:527–534 https://doi.org/10.1093/humrep/deq374

Vanneste E *et al.* (2009) **Chromosome instability is common in human cleavage-stage embryos** *Nat Med* **15**:577–583 https://doi.org/10.1038/nm.1924

Vázquez-Diez C, Paim LMG, FitzHarris G (2019) **Cell-Size-Independent Spindle Checkpoint Failure Underlies Chromosome Segregation Error in Mouse Embryos** *Current Biology* **29**:865–873 https://doi.org/10.1016/j.cub.2018.12.042

Vera-Rodriguez M, Chavez SL, Rubio C, Pera RAR, Simon C (2015) **Prediction model for aneuploidy in early human embryo development revealed by single-cell analysis** *Nat Commun* **6** https://doi.org/10.1038/ncomms8601

Victor AR, Tyndall JC, Brake AJ, Lepkowsky LT, Murphy AE, Griffin DK, McCoy RC, Barnes FL, Zouves CG, Viotti M (2019) **One hundred mosaic embryos transferred prospectively in a single clinic: exploring when and why they result in healthy pregnancies** *Fertil Steril* **111**:280–293 https://doi.org/10.1016/j.fertnstert.2018.10.019

Viotti M *et al.* (2021) **Using outcome data from one thousand mosaic embryo transfers to formulate an embryo ranking system for clinical use** *Fertil Steril* **115**:1212–1224 https://doi.org/10.1016/j.fertnstert.2020.11.041

Voullaire L, Slater H, Williamson R, Wilton L (2000) **Chromosome analysis of blastomeres from human embryos by using comparative genomic hybridization** *Hum Genet* **106**:210–7

Wang C, Zhang J, Yin J, Gan Y, Xu S, Gu Y, Huang W (2021) **Alternative approaches to target Myc for cancer treatment** *Signal Transduction and Targeted Therapy* **6**:1–14 https://doi.org/10.1038/s41392-021-00500-y

Wells D, Delhanty JD (2000) **Comprehensive chromosomal analysis of human preimplantation embryos using whole genome amplification and single cell comparative genomic hybridization** *Mol Hum Reprod* **6**:1055–62

Williams BR, Prabhu VR, Hunter KE, Glazier CM, Whittaker CA, Housman DE, Amon A (2008) **Aneuploidy affects proliferation and spontaneous immortalization in mammalian cells** *Science* **322**:703–709 https://doi.org/10.1126/SCIENCE.1160058

Yan L *et al.* (2013) **Single-cell RNA-Seq profiling of human preimplantation embryos and embryonic stem cells** *Nat Struct Mol Biol* **20**:1131–1139 https://doi.org/10.1038/nsmb.2660

Yang M, Rito T, Metzger J, Naftaly J, Soman R, Hu J, Albertini DF, Barad DH, Brivanlou AH, Gleicher N (2021) **Depletion of aneuploid cells in human embryos and gastruloids** *Nat Cell Biol* **23**:314–321 https://doi.org/10.1038/s41556-021-00660-7

Esteki M Zamani *et al.* (2019) **In vitro fertilization does not increase the incidence of de novo copy number alterations in fetal and placental lineages** *Nat Med* https://doi.org/10.1038/s41591-019-0620-2

Zanetti M, Rodvold JJ, Mahadevan NR (2016) **The evolving paradigm of cell-nonautonomous UPR-based regulation of immunity by cancer cells** *Oncogene* **35**:269–278 https://doi.org/10.1038/ONC.2015.108

Zhang M, Cheng L, Jia Y, Liu G, Li C, Song S, Bradley A, Huang Y (2016) **Aneuploid embryonic stem cells exhibit impaired differentiation and increased neoplastic potential** *EMBO J* **35**:2285–2300 https://doi.org/10.15252/EMBJ.201593103

Zhu J, Tsai HJ, Gordon MR, Li R (2018) **Cellular Stress Associated with Aneuploidy** *Dev Cell* https://doi.org/10.1016/j.devcel.2018.02.002

Author information

Marius Regin

Research Group Genetics Reproduction and Development, Faculty of Medicine and Pharmacy, Vrije Universiteit Brussel, Brussels, Belgium
ORCID iD: 0000-0001-7053-7354

Yingnan Lei

Research Group Genetics Reproduction and Development, Faculty of Medicine and Pharmacy, Vrije Universiteit Brussel, Brussels, Belgium

Edouard Couvreu De Deckersberg
Research Group Genetics Reproduction and Development, Faculty of Medicine and Pharmacy, Vrije Universiteit Brussel, Brussels, Belgium
ORCID iD: 0000-0002-1199-4536

Charlotte Janssens
Research Group Genetics Reproduction and Development, Faculty of Medicine and Pharmacy, Vrije Universiteit Brussel, Brussels, Belgium

Anfien Huyghebaert
Research Group Genetics Reproduction and Development, Faculty of Medicine and Pharmacy, Vrije Universiteit Brussel, Brussels, Belgium

Yves Guns
Brussels IVF, Universitair Ziekenhuis Brussel, Brussels, Belgium

Pieter Verdyck
Vrije Universiteit Brussel (VUB), Universitair Ziekenhuis Brussel (UZ Brussel), Clinical Sciences, Research Group Genetics Reproduction and Development, Centre for Medical Genetics, Brussels, Belgium
ORCID iD: 0000-0002-0243-8650

Greta Verheyen
Brussels IVF, Universitair Ziekenhuis Brussel, Brussels, Belgium
ORCID iD: 0000-0003-4677-2084

Hilde Van de Velde
Research Group Genetics Reproduction and Development, Faculty of Medicine and Pharmacy, Vrije Universiteit Brussel, Brussels, Belgium, Brussels IVF, Universitair Ziekenhuis Brussel, Brussels, Belgium

Karen Sermon[#]
Research Group Genetics Reproduction and Development, Faculty of Medicine and Pharmacy, Vrije Universiteit Brussel, Brussels, Belgium
ORCID iD: 0000-0002-2311-9034

[#]These authors contributed equally to this work

Claudia Spits[#]
Research Group Genetics Reproduction and Development, Faculty of Medicine and Pharmacy, Vrije Universiteit Brussel, Brussels, Belgium
ORCID iD: 0000-0002-0187-5138

For correspondence: Claudia.Spits@vub.be
[#]These authors contributed equally to this work

Editors

Reviewing Editor
Carlos Simon
Foundation Carlos Simon and Valencia University, Valencia, Spain

Senior Editor
Wei Yan
The Lundquist Institute, Torrance, United States of America

Reviewer #2 (Public review):

A high fraction of cells in early embryos carry aneuploid karyotypes, yet even chromosomally mosaic human blastocysts can implant and lead to healthy newborns with diploid karyotypes. Previous studies in other models have shown that genotoxic and proteotoxic stresses arising from aneuploidy lead to the activation of the p53 pathway and autophagy, which helps eliminate cells with aberrant karyotypes. These observations have been here evaluated and confirmed in human blastocysts. The study also demonstrates that the second lineage and formation of primitive endoderm are particularly impaired by aneuploidy.

Comments on revisions:

The authors have addressed the critical issues sufficiently. In particular, they improved the data analysis and added additional data from embryonal samples.

https://doi.org/10.7554/eLife.88916.2.sa2

Reviewer #3 (Public review):

This study provides valuable insights into the cellular responses to complex aneuploidy in human preimplantation embryos. The authors have significantly expanded their sample size and conducted additional analysis and experiments to address previous concerns. The revised manuscript presents stronger evidence for gene dosage-dependent effects of aneuploidy on stress responses and lineage segregation. Overall, the findings contribute important knowledge to our understanding of how human embryos respond to chromosomal abnormalities.

Overall, the revision has substantially improved the manuscript and addressed the major concerns raised in the initial review.

https://doi.org/10.7554/eLife.88916.2.sa1

Author response:

The following is the authors' response to the original reviews.

> ***eLife Assessment***
>
> *This study has uncovered some important initial findings about cellular responses to aneuploidy through analysis of gene expression in a set of donated human embryos. While the study's findings are in general solid, some experiments lack statistical power due to small sample sizes. The authors should try to get much more insight with their data highlighting the novel findings.*

We thank the editor for considering our manuscript for publication at *elife*, and for the helpful and thorough reviews of our work. Based on the suggestions of the reviewers, we have carried out additional experiments, expanded the sample size and reanalyzed the data. This has resulted in a thoroughly revised manuscript and much improved work, which we are convinced meets the requirements to be published as a version of record. Of note, the experiments for the revision required the support by 2 additional researchers from our lab which are now coauthors.

These are the main changes made to the initial manuscript:

(1) The RNA-seq data (Figures 1+2) is now FDR corrected and been reanalyzed. This has not affected the initial observations on the activation of p53 and apoptosis in aneuploid human embryos, as well as that the transcriptomic changes are driven by gene dosage effects.

(2) We have included the transcriptome analysis of reversine-treated embryos in the supplementary data.

(3) For validation of novel findings such as the presence of DNA-damage and the expression of DRAM1 in aneuploid embryos, we now include the stainings of 30 human blastocysts (Figure 3o-t). We found absence of DNA-damage in aneuploid embryos and that DRAM1 is increased in the TE but not the ICM of aneuploid embryos.

(4) We re-analyzed the co-expression of CASP8/HSP70 in reversine-embryos as suggested by reviewer 1 and found that both proteins tend to be co-expressed.

(5) We have added a new analysis of NANOG expression (Figure 4a,b) of the embryos used in Figure 3o-t and have found retention of NANOG protein in both the TE and ICM.

(6) We have added 6 euploid and 4 aneuploid embryos to Figure 4l-s, which support the conclusions on the absence of autophagy activation in the ICM and failure of PrE formation in aneuploid embryos.

(7) We have significantly changed the layout of the figures, revised the supplementary tables, added source data files and rewritten the discussion.

Regarding the sample size of the study, it is important to emphasize that human embryos are ethically sensitive material and that those with the specific genetic content we used in this study are rare, limiting our ability to expand the sample size. For the revision, we have added 40 human blastocysts to our initial 85 embryos. Compared to similar and high-quality studies using human embryos, our study shows a relatively large sample size (n=125): Victor *et al.* 2021: 30 human blastocysts for immunostainings1; Martin *et al.* 2023: 14 human blastocysts2; Martin *et al.* 2024: 64 human blastocysts3; Domingo-Muelas *et al.* 2023: 23 human blastocysts4.

> ***Public Reviews:***
>
> ***Reviewer#1(PublicReview):***
>
> *This study investigated an important question in human reproduction: why most fully aneuploid embryos is incompatible with normal fetal development. Specifically, the authors investigated the cellular responses to aneuploidy through analysis of gene expression in a set of donated human blastocysts. The samples included uniform aneuploid embryos of meiotic origin and mosaic aneuploid embryos from the SAC inhibitor reversine treatment. The authors relied mainly on low-input RNA sequencing and immunofluorescence staining. Pathway analysis with RNA-seq data of trophectoderm cells suggested activation of p53 and possibly apoptosis, and this cellular signature appeared to be stronger in TE cells with a higher degree of aneuploidy.*

> *Immunostaining also found some evidence of apoptosis, increased expression of HSP70 and autophagy in some aneuploid cells. With combinational OCT4 and GATA4 as lineage markers, it appeared that aneuploidy could alter the second lineage segregation and primitive endoderm formation in particular.*
>
> *Although this study is largely descriptive, it generated valuable RNA-seq data from a set of aneuploid TE cells with known karyotypes. Immunostaining results in general were consistent with findings in mouse embryos and human gastruloids.*

We thank the reviewer for the thorough evaluation of our manuscript. We have implemented most of the suggestions, which have further strengthened the original findings.

> *While there is a scarcity of human embryo materials for research, the lack of single cell level data limits further extension of the presented data on the consequences of mosaic embryos.*

We did not include single cell RNA-seq data of mosaic human embryos in our study because we focused on embryos diagnosed with complex meiotic abnormalities. Our hypothesis was that the cellular consequences of aneuploidy would be strongest in this type of aneuploidies and most evident to identify and would allow us to provide a basis for the mechanisms of elimination of aneuploid cells in human embryos. In the manuscript (lines 596-626) we acknowledge the limitations of the extrapolation of our results to mosaic embryos.

> *A major concern is that the gene list used for pathway analysis is not FDR controlled. It is also unclear how the many plots generated with the "supervised approach" were actually performed.*

We agree with the concerns about the fact that our differential expression gene list was not FDR but p-value ranked. We followed the suggestion of the reviewer and revised the RNAseq analysis and focused primarily on pathway analysis. We have also added the comparison between aneuploid and reversine treated embryos to the supplementary data and expanded the analysis of high dosage and low dosage embryos. Importantly, the new analysis has not changed the original finding that aneuploid embryos show hallmarks of p53 activation and apoptosis, and that these effects are gene dosage dependent. The manuscript now includes two completely revised and new figures 1 and 2.

Since we discarded the data generated from our previous approach, we do not use the term supervised approach anymore.

> *The authors also appear to have ignored the possibility that high-dosage group could have a higher mitotic defect.*

This is indeed a possibility. In the discussion (lines 504-508) we have now incorporated the notion that the high dosage embryos could have higher mitotic defects, although our data cannot provide any evidence for this. Of note, the gene expression data shows that all aneuploid embryos (including low dosage and reversine embryos) equally show an enrichment for mitotic spindle pathway genes.

> *Assuming a fully aneuploid embryo, why do only some cells display p53 and autophagy marker?*

This is a very good question, on which we can only speculate, but the answer likely lies in the diversity across cells of the same embryo.

Even in genetically homogenous tissues and cell cultures, individual cells can exhibit different levels of stress responses, such as p53 activation and apoptosis. This variation may be influenced by the local cellular environment, stochastic gene expression, or differences in cell cycle stages. Other studies on fully aneuploid human embryos could also not detect apoptotic responses in every cell1,3.

For instance, p53 activation differs even between cells that have a similar number of DNA breaks, and this activation is influenced by both cell-intrinsic factors and previous exposure to DNA damage5.

Cell cycle tightly regulates the response of cells to different stressors. For instance, cells in G1 or S-phase might be more sensitive to apoptosis signals6, while those in G2/M might escape this response temporarily7. Autophagy is more induced in G1 and S phases, with reduced activity in G2 and M phases8.

Individual cells may also have different levels of success in the activation of the compensatory pathways, including the unfolded protein response, autophagy, or changes in metabolism, resulting in some cells adapting better than others.

The expression of p53 and the sensitivity to apoptosis could also be influenced by epigenetic differences between cells, which may alter their transcriptional response to aneuploidy. Even in a genetically identical population, cells can have different epigenetic landscapes, leading to heterogeneous gene expression patterns.

> *The conclusion about proteotoxic stress was largely based on staining of HSP70. It appears from Figure 3 d,h that the same cells exhibited increased HSP70 and CASP8 staining. Since HSP70 is known to have anti-apoptotic effect, could the increased expression of Hsp70 be an anti-apoptotic response?*

Our conclusion about proteotoxic stress was not solely based on HSP70 expression. We also stained for LC3B and p62, which are markers for autophagy and when highly expressed indirectly point towards underlying proteotoxic stress in the cells.

We reanalyzed the imaging of the stainings in the reversine-treated embryos, and found that the same cells were positive for both HSP70 and CASP8 staining while the minority was single positive (shown now in Figure 3k,l).

HSP70 does indeed not only unfold misfolded and aggregated proteins but does also have a function during cell survival and apoptosis9. HSP70 has been for instance found to inhibit the cleavage of Bid through active CASP8 within the extrinsic apoptosis pathway10. It is thus possible that it temporarily plays this role, and we have acknowledged this in the discussion (lines 623-626). On the other hand, the evidence points at an active apoptosis in the TE, with concomitant cell loss, so if HSP70 is indeed having an anti-apoptotic effect, it is having a limited impact.

> ***Reviewer #2 (Public Review):***
>
> *A high fraction of cells in early embryos carry aneuploid karyotypes, yet even chromosomally mosaic human blastocysts can implant and lead to healthy newborns with diploid karyotypes. Previous studies in other models have shown that genotoxic and proteotoxic stresses arising from aneuploidy lead to the activation of the p53 pathway and autophagy, which helps eliminate cells with aberrant karyotypes. These observations have been here evaluated and confirmed in human blastocysts. The study also demonstrates that the second lineage and formation of primitive endoderm are particularly impaired by aneuploidy.*

> *This is a timely and potentially important study. Aneuploidy is common in early embryos and has a negative impact on their development, but the reasons behind this are poorly understood. Furthermore, how mosaic aneuploid embryos with a fraction of euploidy greater than 50 % can undergo healthy development remains a mystery. Most of our current information comes from studies on murine embryos, making a substantial study on human embryos of great importance. However, there are only very few new findings or insights provided by this study. Some of the previous findings were reproduced, but it is difficult to say whether this is a real finding, or whether it is a consequence of a low sample number. The authors could get much more insight with their data.*

We thank the reviewer for the thorough evaluation of our manuscript and the valuable suggestions made in the private recommendations. We have expanded the sample size and have carried out additional experiments that have significantly improved the manuscript.

> ***Recommendations for the authors:***
>
> ***Reviewer #1 (Recommendations For The Authors):***
>
> *(1) Instead of using cut off to generate a list, the authors could just rank the entire detected transcriptome for GSEA. This method fits better the authors' intentions of "primarily focused on pathway analysis." The cut-off value "-log10(p-value)<0.05" is not correct. As we can see from the PCA plot, one would not expect many cut off defined DEGs at all. The most obvious transcriptome change is dosage dependent, as the authors cleared showed with InferCNV.*

We thank the reviewer for this suggestion and agree that this was an important concern of the study. We have entirely revised the RNA-seq analysis based on the proposed approach (Figure 1 and 2, Supplementary Figure 1). Also, we have included the analysis of aneuploid versus reversine treated embryos, which has allowed us to determine the differences between naturally occurring chromosomal abnormalities and those that are induced using reversine (Supplementary Figure 1).

We first performed differential gene expression analysis using DESEq2 with a cut-off value for significantly differentially expressed genes of | log2FC | > 1 and an FDR < 0.05. Based on the PCAs and the low number of differentially expressed genes for all comparisons, besides high dosage versus euploid embryos, we focussed primarily on pathway analysis.

For that, based on the reviewer's suggestion, we generated a ranked gene list using the GSEA software (version 4.2.2, MSigDatabase) based on the normalized count matrix of the whole transcriptome that was detected after differential gene expression. The ranked gene list was then subjected to the *run GSEA* function, and we searched the Hallmark and C2 library for significantly enriched pathways. Thus, we could generate normalized enrichment scores, allowing us to predict whether a pathway is activated or suppressed. The details of the new analysis are described in the Material and Methods section (lines 220-232). Significance was determined using a cut-off value of 25% FDR. This cut-off is proposed in the user guide of the GSEA (https://www.gsea-msigdb.org/gsea/doc/GSEAUserGuideTEXT.htm) especially for incoherent gene expression datasets, as suggested by our PCAs, which allows for hypothesis driven validation of the dataset.

Indeed, we found that the most important transcriptome changes are aneuploidy dosage dependent. High dosage embryos show signatures of cellular unfitness, while low-dosage embryos still seem to activate survival pathways (lines 349-364).

This new analysis did not only increase robustness of our results but also introduced novel findings, which pave the road for future studies.

The validity of our findings is supported by recent work by the Zernicka-Goetz lab. We found that hypoxia is upregulated in low dosage human aneuploid TE cells. In line with our data, the Zernicka-Goetz lab found in a mouse model of low degree chromosomal abnormalities that hypoxia inducible factor 1A (HIF1A) promotes survival of extraembryonic aneuploid cells by reducing levels of DNA damage11.

> *(2) It would be very helpful if the authors could perform co-staining of multiple stress markers to better understand the origins of apoptosis and autophagy cells. In Fig 3d and 3h, it seems that the same reversine treated embryo was stained with CASP8, LC3B and HSP70. Is there any correlation between CASP8 and HSP70 at the single cell level? Is there any correlation between p53 and LC3B as the authors suggested, possibly through DRAM1?*

We decided to use the complex aneuploid embryos that were left at our facility for the validation of novel findings such as upregulation of DRAM1 and presence and consequences of DNA damage in aneuploid embryos. As suggested by the editor and the other reviewer we also added embryos to existing datasets to increase the sample size where necessary. Therefore, we did not include other co-staining's of multiple stress markers.

Following the reviewer's suggestion, we reanalyzed the existing stainings and evaluated whether there is a correlation between CASP8 and HSP70 at the single cell level. The reversine-treated embryos were the only embryo group that was co-stained for both CASP8 and HSP70. We quantified the percentage of cells that were single or double positive for CASP8 and HSP70 and found a higher proportion of double positive cells than to single positives. Therefore, we concluded that there is indeed a correlation between both proteins at the single cell level in reversine-treated embryos and included this data in Figure 3k,l.

During the experiments for the revision, we found that the DRAM1 protein was upregulated in the cytoplasm of TE cells but not in the ICM of aneuploid embryos (Figure 3s,t), which validates the findings of the gene expression analysis. This data also supports our findings that autophagy is active in aneuploid TE cells while not significantly increased in aneuploid pluripotent ICM cells. Unfortunately, we could not stain LC3B and DRAM1 in the same embryo because the antibodies were raised in the same species.

> *(3) While " the possibilities for functional studies and lineage tracing experiments in human embryos are very limited," the authors can leverage in silico modelling (ie, PMID: 28700688) to address the roles of aneuploidy in blastocyst formation and development. Is there any selfregulating mechanism underlying the ratios of PrE and EPI? Is apoptosis of ICM cells a natural process during PrE formation (PMID: 18725515)?*

It is a very interesting proposal to use *in silico* modelling to address the roles of aneuploidy during human blastocyst formation and lineage segregation. Although this type of analysis would yield very important insights, we are not able to address this point of the revision due to lack of expertise for this type of analysis in our group, requiring setting up a collaboration with experts in this field. In the discussion we proposed that future studies can leverage our data to be carried out in *silico* modelling and cited the proposed article (lines 608-610).

On the second part of the question, we would like to discuss the differences between mouse and human embryo studies. Parts of this were included in the discussion on the possible mechanisms of PrE elimination.

> *Is there a self-regulating mechanism for EPI/PrE formation?*

To extrapolate the knowledge on mouse development to human it is important to bear in mind that (1) human embryos are outbred, as compared to inbred super-fertile laboratory mouse strains and (2) the embryos are donated to research by subfertile couples, which could compromise the EPI/PrE ratios. For instance, Chousal and colleagues found that poor quality blastocysts have a reduced number of PrE cells12. In human embryos the proportion EPI and PrE cells is indeed highly variable (20%-60%) and while the number of EPI cells does not increase between dpf6 and 7, the number of PrE cells does grow13. We found a similar variable number of EPI and PrE in our study on the lineage segregation mechanisms in good quality human embryos, with an absolute number of EPI of 12.1±6.5 cells and 8.4±3.44 PrE cells14.

By comparison, in late mouse blastocysts, the ratio EPI/PrE cells is consistent (2/3)15. Overall, self-regulating mechanisms in the human embryo are not yet studied in detail due to the lack of possible functional testing.

> *Is apoptosis a natural process during PrE formation?*

Yes, in mice apoptosis is a natural process during PrE formation to eliminate misallocated cells of the inner cell mass through cell competition16,17. Yet, in the human embryo there is no evidence of such mechanisms. Although apoptosis is present even in human blastocysts of good quality18, the origin of such apoptotic cells is now still shown, although suboptimal culture conditions are known to increase cellular fragmentation19. Conversely, our data and that of others1,2 supports the notion that the pluripotent inner cell mass in human embryos is more resistant to apoptosis than the trophectoderm, even in karyotypically aberrant cells.

> *(4) The "count tables generated from the raw data files" could not be found in the source data files.*

This slipped to our attention, we have added now the count tables to the source data files. Our apologies.

> *(5) Citations on aneuploidy literature were not done in a fully scholarly manner. It appears that authors selectively cite previous papers that are in support of their hypothesis but left out those with alternative conclusions.*

We apologize if we missed any literature that contradicts our findings, it is not intentional. We would be grateful if the reviewer could provide such references.

In the manuscript we describe the alignment and differences of key findings with several studies (listed below) and the limitations of our study are extensively described in lines 596626.

Our findings align with other work on these aspects:

- RNA-sequencing data2,20–26

- Gene dosage effects drive the transcriptome of the aneuploid human embryo27,28

- Aneuploid cells are cleared by sustained proteotoxic stress followed by p53 activation, autophagy and eventually apoptosis29–37.

- p53 is active in constitutional aneuploid cells38

- The ICM is less sensitive to apoptosis1,2

Our findings differ with other work on these points:

- p53 activation is independent from DNA-damage39

- p53 is active in constitutional aneuploid cells40,41

- Apoptosis is only present in the aneuploid TE of aneuploid cells in the embryo29,30,42

> ***Reviewer #2 (Recommendations For The Authors):***
>
> *Comments:*
>
> *(1) The main problem is that there is no substantial novelty. The authors look at previously identified factors affected by chromosome gains and losses, but none of the new one from their analysis. Anything what could be potentially novel is not carefully analyzed (e.g. the difference between reversine-treated and aneuploid samples, or new potential candidates) or explained. This is really a pity.*

In the revision, we have further elaborated on the DNA damage aspect by staining for DNA double-stranded breaks and have validated DRAM1 as an activated downstream effector of p53. We have also added the analyses of the gene-expression of the reversine-treated embryos.

> *(2) Some of the general statements on aneuploidy are confusing and often borderline generalized. E.g. introduction line 106: "If this (proteotoxic stress) remains unresolved by the activation of autophagy..." I am not aware of any publication suggesting that autophagy resolves proteotoxic stress in aneuploid cells. Citations that replication stress causes DNA damage in aneuploid cells are wrong. This link was first shown by Passerini et al. in 2016. etc.*

We have clarified these statements in the introduction and added the proposed citations on replication stress that causes DNA damage in aneuploid cells (lines 95-108).

> *(3) In the figures the authors show a representative image of aneuploid and diploid embryos. Given the aneuploid embryos have widely different karyotypes, it would be important to clarify which of the embryos has been actually shown. Similarly, in the heat maps it is not clear which line is which embryo. This would be very useful.*

We added the karyotypes of the aneuploid embryos to the images in figure 3 and 4. Since the heatmaps were removed from the figures we added the karyotypes to the PCAs in all figures.

> *(4) The authors constantly state that aneuploid embryo accumulate more DNA damage, which is supported by some of their observations, e.g. the DNA damage response is upregulated. It would be great if they would validated this statements with testing some markers for DNA damage.*

We agree with the reviewer that this was an important point and addressing it has revealed that our initial assumption was incorrect and has provided new interesting findings. From the revised RNA-seq analysis, we found only one pathway (DNA damage response TP53) to be activated in all aneuploid embryos (Fig.1e). The ATM pathway was also activated specifically in high-dosage embryos. Following this, we set to test if DNA damage was indeed increased in aneuploid embryos by staining for DNA double strand breaks with gH2AX.

First, we investigated the gH2AX expression in 5dpf embryos in which we induced DNAdamage with Bleomycin. We compared 6 untreated versus 6 Bleomycin treated human embryos (Fig. 3m) and found that gH2AX foci were rarely present in the untreated embryos and that all cells of the treated embryos showed a pan-nuclear gH2AX staining.

Second, we compared the presence of gH2AX foci in the TE (NANOG negative cells), ICM (NANOG positive cells) and the whole embryo of 7 euploid versus 11 aneuploid embryos. Interestingly, we found no differences in the number of gH2AX foci or pan-nuclear gH2AX nuclei between euploid and aneuploid embryos (Fig 3o). When dividing our aneuploid embryos into high and low dosage embryos we could also not account for differences. Our data now suggests that complex aneuploid human embryonic cells of meiotic origin do not contain more DNA-double strand breaks, precluding DNA-damage as the source of p53 activation. Last, in our previous experiment we found that phosphorylated S15p53 is increased in aneuploid embryos, supporting an active p53 pathway as suggested by our transcriptomic data. Since we could not find DNA-damage in aneuploid human embryos we speculate that p53 is phosphorylated on Serine15 through metabolic stress as suggested by Jones and colleagues43. We also argue that proteotoxic stress might induce p53 expression as proposed by Singla and colleagues29.

> *(5) The source of embryos is only partially described in a figure legend. This should be expanded and described in the Materials and Methods section. The embryos are named, but this is nowhere explained. One can only assume that T is for trisomy and M is for monosomy.*

We have divided the embryos into different experimental series (Experiment 1-4). This is now described in the Material and methods section (lines 157-175). Also, we have added the experiment number of each embryo to the supplementary tables and to the source data. The abbreviation for T = Trisomy and M= Monosomy was initially introduced in the last paragraph of the figure legend of figure 4. We now added it to every panel.

> *(6) Recent works from non-embryonic cells suggest that the cellular response to monosomy is different than the response to trisomy. Did the authors try to test this possible difference? For example, one could compare embryos M174/21, M2/19 and M17 with T2/10, T10/22 and T1/15/18/22.*

We thank the reviewer for pointing this out. Our RNA-seq. dataset consisted of three embryos that contained trisomies only and four embryos that contained monosomies only. When reanalyzing our data we found different transcriptomic responses between monosomic only and trisomic only cells. Compared to euploid cells, monosomy only cells activate mainly the p53pathway and protein secretion while translation, DNA replication, cell cycle G1/S, DNA synthesis and processing of DNA double strand breaks were inhibited. Trisomy only cells show activated oxidative phosphorylation, ribosome and translation while protein secretion, apoptosis and cell cycle are inhibited. These differences were confirmed by testing transcriptomic differences between trisomic versus monosomic cells. Our results are similar to studies on human embryos20,26 and other monosomic and trisomic cell lines44,45. However, the interpretation of these results is very limited by the small sample size and the comparison of monosomies and trisomies of different chromosomes. Thus, we decided to keep this analysis out of the manuscript.

Author response image 1.

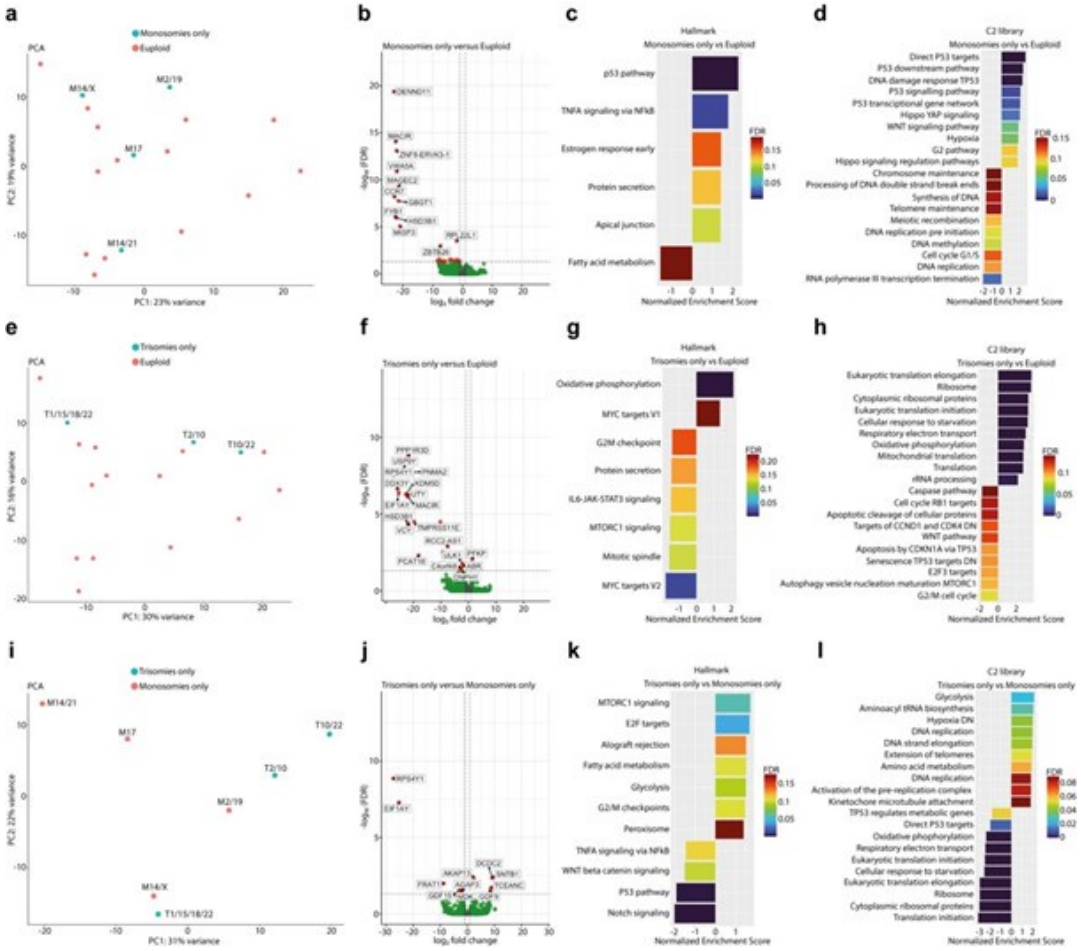

On the protein level, next to the small sample size, our results were also limited by the fact that not all embryos were stained with the same combinations of antibodies. LC3B was the only protein for which all embryos were immunostained. Thus, other protein data could not be re-analyzed due to even lower sample sizes.

Below we have separated the LC3B puncta per cell counts into euploid, trisomies only, monosomies only and all other aneuploid embryos. We performed a Kruskal Wallis test with multiple comparisons. It is worth noticing that the difference between euploid and monosomies only (and those that contained both) was statistically significant, while the difference between euploid vs trisomies only and trisomies only vs monosomies only was not statistically significant. These differences contradict the studies on monosomic cell lines that found that proteotoxic stress and autophagy are not present and specific to trisomic cell lines. Here we also decided to keep this specific protein expression analysis out of the manuscript due to the above-mentioned limitations.

Author response image 2.

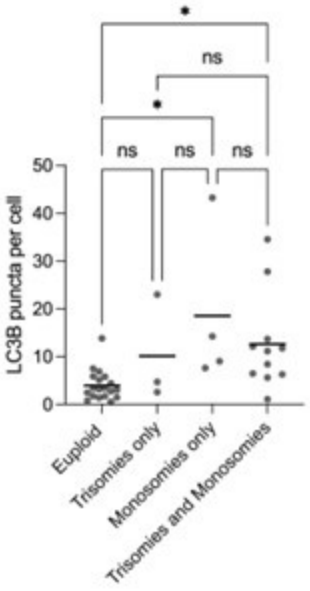

> *(7) Line 329: "a trisomy 12 meiotic chromosomal abnormality in one reversine-treated embryo." What does it mean? Why meiotic chromosomal abnormality when the reversine treatment was administered 4 days after fertilization? In the discussion, the authors state "presumed meiotic," but this should be discussed and described more clearly.*

Since reversine induces mitotic abnormalities of different types leading to chromosomally mosaic embryos, we could not identify these induced abnormalities using inferCNV on the RNAseq of TE biopsies of said embryos. However, we were not aware of the karyotype of the embryos that were used for these experiments, as they were thawed after they had been cryopreserved at day 3 of development and had not been subjected to genetic testing. This makes it possible that some of those embryos we used for the reversine experiments in fact carried endogenously acquired meiotic and mitotic chromosomal abnormalities. Since we are only able to detect by inferCNV aneuploidies homogeneously present in the majority of the cells of the sequenced biopsy, we only picked up this trisomy 12. It is possible that this was not a meiotic abnormality but a miotic one originating at the first cleavage and present at a high percentage of cells in the blastocyst. At any rate, the exact origin of this aneuploidy has no further implications for the results of the study. We clarified this in the manuscript (lines 310-315).

> *(8) Line 422: "The gene expression profiles suggest that the accumulation of autophagic proteins in aneuploid embryos is caused by increased autophagic flux due to differential expression of the p53 target gene DNA Damage Regulated Autophagy Modulator-1 (DRAM1), rather than by inhibition of autophagy (Supplementary Table 2)." This is highly speculative, as the authors do not have any evidence to support this statement.*

To validate this finding we have now stained 7 euploid and 11 aneuploid embryos with a DRAM1 antibody. We found DRAM1 protein to be significantly enriched in the cytoplasm of TE cells but not in the ICM of aneuploid embryos when comparing with euploid embryos (Fig. 3s,t). This data is consistent with the finding that autophagy is increased in the TE and not the ICM of aneuploid human embryos. (Fig 4l-o). Potential implications of DRAM1 expression have been mentioned in the discussion.

> *(9) The figure legends are confusing. They are mixed up with the methods and some key information are missing.*

We revised all figure legends accordingly and removed the experimental set-up figures from the manuscript to reduce any confusion. The methods section was revised and expanded.

> *(10) In Figure 1, what is the difference between "activated" and "deregulated"?*

Since we analyzed our RNA-seq dataset with the method proposed by reviewer 1 we now generated normalized enrichment scores. The terms activated and deregulated are thus not present anymore.

> *(11) The p62 images are not really clear. There might be more puncta (not obvious, though), but the staining intensity seems lower in the representative images.*

We do not agree with the reviewer that there might be more p62 puncta (purple), however, we agree that it was not clearly visible from the pictures. Below we show an example of the counting mask (in green) of the aneuploid embryo from figure 3i, where one can clearly appreciate that all the puncta are captured by the counting mask. In this case, the software counted 1704 puncta. To further clarify, we now added a zoom of a randomly chose ROI of the p62 staining's to figure 3i.

Author response image 3.

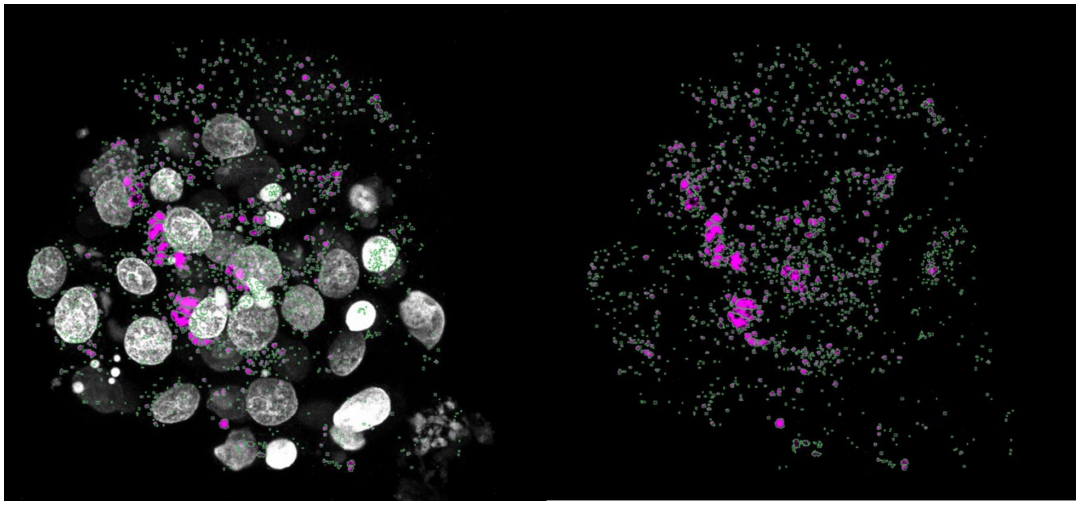

> *(12) The authors claim that there are differences between lineages in response to aneuploidy, such as autophagy not being activated in the OCT4+ lineage, etc. However, the differences are very small and based on a small number of embryos. It is difficult to draw far-reaching conclusions based on a small number of experiments (Fig. 4n-r). The authors also claim in the Abstract that they demonstrated "clear differences with previous findings in the mouse", which are however difficult to identify in the text.*

We agree with the reviewer that our conclusions on figures 4l-o were based on a small number of embryos. We have increased as much as possible the sample size. This is challenging due to the constrictions in accessing human embryos, and especially the limited number of embryos with meiotic complex aneuploidy. We have performed immunostainings for LC3B, OCT4 and GATA4 of six additional euploid and four additional aneuploid human

embryos. This did not change our overall findings that aneuploid embryos upregulate autophagy in the TE rather than the ICM (Figure 4l-o). After the inclusion of additional embryos, we removed our speculation from the manuscript that autophagy is present in ICM cells of already differentiated cells towards EPI/PrE.

We have rephrased the abstract to state that we highlight a few differences with previous findings in the mouse. Here we focused especially on the different transcriptomic response of reversine treated embryos, that aneuploid mouse embryos do not seem to suffer from lineage segregation errors and that the ICM of aneuploid human embryos lacks apoptosis while aneuploid mouse embryos show elimination from the EPI. Likewise, we highlighted the similar stress responses and that we could give novel insights into p53 mediated autophagy and apoptosis activation through DRAM1 in aneuploid TE cells but not the ICM.

> *(13) The text needs thorough editing - long sentences, typos, and grammar errors are frequent. Punctuation is largely missing.*

We have revised the text.

References

(1) Victor, A. R. *et al.* One hundred mosaic embryos transferred prospectively in a single clinic: exploring when and why they result in healthy pregnancies. *Fertil Steril* 111, 280–293 (2019).

(2) Martin, A. *et al.* Mosaic results after preimplantation genetic testing for aneuploidy may be accompanied by changes in global gene expression. *Front Mol Biosci* 10, 264 (2023).

(3) Martín, Á. *et al.* Trophectoderm cells of human mosaic embryos display increased apoptotic levels and impaired differentiation capacity: a molecular clue regarding their reproductive fate? *Human Reproduction* 39, 709–723 (2024).

(4) Domingo-Muelas, A. *et al.* Human embryo live imaging reveals nuclear DNA shedding during blastocyst expansion and biopsy. *Cell* 186, 3166-3181.e18 (2023).

(5) Loewer, A., Karanam, K., Mock, C. & Lahav, G. The p53 response in single cells is linearly correlated to the number of DNA breaks without a distinct threshold. *BMC Biol* 11, 1–13 (2013).

(6) Kim, H., Watanabe, S., Kitamatsu, M., Watanabe, K. & Ohtsuki, T. Cell cycle dependence of apoptosis photo-triggered using peptide-photosensitizer conjugate. *Scientific Reports 2020 10:1* 10, 1–8 (2020).

(7) Pollak, N. *et al.* Cell cycle progression and transmitotic apoptosis resistance promote escape from extrinsic apoptosis. *J Cell Sci* 134, (2021).

(8) Neufeld, T. P. Autophagy and cell growth--the yin and yang of nutrient responses. *J Cell Sci* 125, 2359–2368 (2012).

(9) Lanneau, D. *et al.* Heat shock proteins: essential proteins for apoptosis regulation. *J Cell Mol Med* 12, 743 (2008).

(10) Gabai, V. L., Mabuchi, K., Mosser, D. D. & Sherman, M. Y. Hsp72 and Stress Kinase cjun N-Terminal Kinase Regulate the Bid-Dependent Pathway in Tumor Necrosis Factor-Induced Apoptosis. *Mol Cell Biol* 22, 3415 (2002).

(11) Sanchez-Vasquez, E., Bronner, M. E. & Zernicka-Goetz, M. HIF1A contributes to the survival of aneuploid and mosaic pre-implantation embryos. *bioRxiv* 2023.09.04.556218 (2023) doi:10.1101/2023.09.04.556218.

(12) Chousal, J. N. *et al.* Molecular profiling of human blastocysts reveals primitive endoderm defects among embryos of decreased implantation potential. *Cell Rep* 43, (2024).

(13) Corujo-Simon, E., Radley, A. H. & Nichols, J. Evidence implicating sequential commitment of the founder lineages in the human blastocyst by order of hypoblast gene activation. *Development (Cambridge)* 150, (2023).

(14) Regin, M. *et al.* Lineage segregation in human pre-implantation embryos is specified by YAP1 and TEAD1. *Human Reproduction* 38, 1484–1498 (2023).

(15) Saiz, N., Williams, K. M., Seshan, V. E. & Hadjantonakis, A. K. Asynchronous fate decisions by single cells collectively ensure consistent lineage composition in the mouse blastocyst. *Nature Communications 2016 7:1* 7, 1–14 (2016).

(16) Plusa, B., Piliszek, A., Frankenberg, S., Artus, J. & Hadjantonakis, A. K. Distinct sequential cell behaviours direct primitive endoderm formation in the mouse blastocyst. *Development* 135, 3081–3091 (2008).

(17) Hashimoto, M. & Sasaki, H. Epiblast Formation by TEAD-YAP-Dependent Expression of Pluripotency Factors and Competitive Elimination of Unspecified Cells. *Dev Cell* 50, 139-154.e5 (2019).

(18) Hardy, K. Apoptosis in the human embryo. *Rev Reprod* 4, 125–134 (1999).

(19) Ramos-Ibeas, P. *et al.* Embryo responses to stress induced by assisted reproductive technologies. *Mol Reprod Dev* 86, 1292–1306 (2019).

(20) Licciardi, F. *et al.* Human blastocysts of normal and abnormal karyotypes display distinct transcriptome profiles. *Sci Rep* 8, 1–9 (2018).

(21) Maxwell, S. M. *et al.* Investigation of Global Gene Expression of Human Blastocysts Diagnosed as Mosaic using Next-generation Sequencing. *Reproductive Sciences* 1–11 (2022) doi:10.1007/s43032-022-00899-x.

(22) Groff, A. F. *et al.* RNA-seq as a tool for evaluating human embryo competence. *Genome Res* 29, 1705–1718 (2019).

(23) Starostik, M. R., Sosin, O. A. & McCoy, R. C. Single-cell analysis of human embryos reveals diverse patterns of aneuploidy and mosaicism. *Genome Res* 30, 814–826 (2020).

(24) Vera-Rodriguez, M., Chavez, S. L., Rubio, C., Pera, R. A. R. & Simon, C. Prediction model for aneuploidy in early human embryo development revealed by single-cell analysis. *Nat Commun* 6, 7601 (2015).

(25) Sanchez-Ribas, I. *et al.* Transcriptomic behavior of genes associated with chromosome 21 aneuploidies in early embryo development. *Fertil Steril* 111, 991-1001.e2 (2019).

(26) Fuchs Weizman, N. *et al.* Towards Improving Embryo Prioritization: Parallel Next Generation Sequencing of DNA and RNA from a Single Trophectoderm Biopsy. *Sci Rep* 9, 1–11 (2019).

(27) Fernandez Gallardo, E. *et al.* A multi-omics genome-and-transcriptome single-cell atlas of human preimplantation embryogenesis reveals the cellular and molecular impact of chromosome instability. *bioRxiv* 2023.03.08.530586 (2023) doi:10.1101/2023.03.08.530586.

(28) Dürrbaum, M. & Storchová, Z. Effects of aneuploidy on gene expression: implications for cancer. *FEBS J* 283, 791–802 (2016).

(29) Singla, S., Iwamoto-Stohl, L. K., Zhu, M. & Zernicka-Goetz, M. Autophagy-mediated apoptosis eliminates aneuploid cells in a mouse model of chromosome mosaicism. *Nat Commun* 11, 1–15 (2020).

(30) Bolton, H. *et al.* Mouse model of chromosome mosaicism reveals lineage-specific depletion of aneuploid cells and normal developmental potential. *Nat Commun* 7, 1– 12 (2016).

(31) Ohashi, A. *et al.* Aneuploidy generates proteotoxic stress and DNA damage concurrently with p53-mediated post-mitotic apoptosis in SAC-impaired cells. *Nat Commun* 6, 1–16 (2015).

(32) Santaguida, S. & Amon, A. Short- and long-term effects of chromosome missegregation and aneuploidy. *Nature Reviews Molecular Cell Biology* vol. 16 473–485 Preprint at https://doi.org/10.1038/nrm4025 (2015).

(33) Santaguida, S., Vasile, E., White, E. & Amon, A. Aneuploidy-induced cellular stresses limit autophagic degradation. *Genes Dev* 29, 2010–2021 (2015).

(34) Chunduri, N. K. & Storchová, Z. The diverse consequences of aneuploidy. *Nature Cell Biology 2019 21:1* 21, 54–62 (2019).

(35) Dürrbaum, M. *et al.* Unique features of the transcriptional response to model aneuploidy in human cells. *BMC Genomics* 15, 139 (2014).

(36) Pan, J.-A., Ullman, E., Dou, Z. & Zong, W.-X. Inhibition of protein degradation induces apoptosis through a microtubule-associated protein 1 light chain 3-mediated activation of caspase-8 at intracellular membranes. *Mol Cell Biol* 31, 3158–70 (2011).

(37) Stingele, S. *et al.* Global analysis of genome, transcriptome and proteome reveals the response to aneuploidy in human cells. *Mol Syst Biol* 8, 608 (2012).

(38) Tang, Y.-C., Williams, B. R., Siegel, J. J. & Amon, A. Identification of aneuploidyselective antiproliferation compounds. *Cell* 144, 499–512 (2011).

(39) Janssen, A., Van Der Burg, M., Szuhai, K., Kops, G. J. P. L. & Medema, R. H. Chromosome segregation errors as a cause of DNA damage and structural chromosome aberrations. *Science* 333, 1895–1898 (2011).

(40) Li, M. *et al.* The ATM-p53 pathway suppresses aneuploidy-induced tumorigenesis. *Proc Natl Acad Sci U S A* 107, 14188–14193 (2010).

(41) Thompson, S. L. & Compton, D. A. Proliferation of aneuploid human cells is limited by a p53-dependent mechanism. *J Cell Biol* 188, 369–381 (2010).

(42) Yang, M. *et al.* Depletion of aneuploid cells in human embryos and gastruloids. *Nat Cell Biol* 23, 314–321 (2021).

(43) Jones, R. G. *et al.* AMP-activated protein kinase induces a p53-dependent metabolic checkpoint. *Mol Cell* 18, 283–293 (2005).

(44) Chunduri, N. K., Barthel, K. & Storchova, Z. Consequences of Chromosome Loss: Why Do Cells Need Each Chromosome Twice? *Cells 2022, Vol. 11, Page 1530* 11, 1530 (2022).

(45) Krivega, M., Stiefel, C. M. & Storchova, Z. Consequences of chromosome gain: A new view on trisomy syndromes. *American Journal of Human Genetics* vol. 109 2126–2140 Preprint at https://doi.org/10.1016/j.ajhg.2022.10.014 (2022).

https://doi.org/10.7554/eLife.88916.2.sa0